Cement and Concrete Research 90 (2016) 52–72

Contents lists available at ScienceDirect

Cement and Concrete Research

journal homepage: www.elsevier.com/locate/cemconres

Diffusivity of saturated ordinary Portland cement-based materials: A critical review of experimental and analytical modelling approaches

Ravi A. Patel [a,b,*], Quoc Tri Phung [a], Suresh C. Seetharam [a], Janez Perko [a], Diederik Jacques [a], Norbert Maes [a], Geert De Schutter [b], Guang Ye [b,c], Klaas Van Breugel [c]

[a] Institute for Environment, Health, and Safety, Belgian Nuclear Research Centre (SCK•CEN), Boeretang 200, B2400 Mol, Belgium
[b] Magnel Laboratory for Concrete Research, Department of Structural Engineering, Ghent University, B9052 Ghent, Belgium
[c] Microlab, Faculty of Civil Engineering and Geosciences, Delft University of Technology, P.O. Box 5048, 2600 GA Delft, The Netherlands

ARTICLE INFO

Article history:
Received 14 December 2015
Received in revised form 14 July 2016
Accepted 20 September 2016
Available online 28 September 2016

Keywords:
B. Microstructure
C. Diffusion
C. Transport properties
D. Cement paste
Analytical models

ABSTRACT

This paper provides a comprehensive overview of existing experimental and modelling approaches to determine effective diffusion coefficients of water saturated ordinary Portland cement-based materials. A dataset for diffusivity obtained from different experimental techniques have been presented for cement paste, mortar and concrete. For cement paste at low porosities, diffusivity reported by different authors varies up to a factor of five and electrical resistivity measurements for low capillary porosity are up to one order of magnitude higher compared to other techniques. Experimental data of mortar and concrete reveals predominant influence of increasing tortuosity due to aggregates and limited influence of interface transition zone. Hence, a particular emphasis has been placed on assessing predictability of diffusivity models for cement paste on a larger dataset collected in this paper. It has been observed that all predictive models have similar level of accuracy and fail to predict electrical resistivity data at low capillary porosity as these models are not calibrated using electrical resistivity data.

Contents

* Corresponding author at: Magnel Laboratory for Concrete Research, Department of Structural Engineering, Ghent University, B9052 Ghent, Belgium.
E-mail addresses: RPatel@sckcen.be (R.A. Patel), QPhung@sckcen.be (Q.T. Phung), SSeethar@sckcen.be (S.C. Seetharam), JPerko@sckcen.be (J. Perko), DJacques@sckcen.be (D. Jacques), NMaes@sckcen.be (N. Maes), Geert.DeSchutter@ugent.be (G. De Schutter), G.Ye@tudelft.nl (G. Ye), K.VanBreugel@tudelft.nl (K. Van Breugel).

http://dx.doi.org/10.1016/j.cemconres.2016.09.015
0008-8846/

Notations

A	Cross-sectional area of the sample
a, a_1, a_2, a_3	Fitting parameter representing coefficients in different models
C	Concentration
C_s	Concentration at the upper compartment (inlet)
C_o	Initial concentration in sample
C_b	Bound concentration
D_a	Apparent diffusivity (often referred to as non-steady state diffusivity in literature)
D_{CSH}	Diffusivity of C-S-H phase
D_e	Effective diffusivity (often referred to as steady-state diffusivity in literature)
D_p	Pore diffusion coefficient
$D_e^p, D_{e,i}^p, D_e^{m/c}$	Effective diffusivity of cement paste in general, cement paste of the i^{th} layer and mortar/concrete respectively
D_e^{itz}, D_e^{agg}	Effective diffusivity of ITZ and aggregates
$D_{e,n}$	Effective diffusivity of the composite with n layer spheres in case of multicoated sphere model
$D_{e,i}$	Effective diffusivity of i^{th} layer in case of transfer matrix method
D_{ea}	Effective diffusivity of an equivalent aggregate system specific to [154] model
D_{hm}	Diffusivity of hypothetical homogeneous medium containing equivalent aggregate system and cement paste specific to [154] model
D_{gp}	Pore water diffusivity in gel pores
D_{HD-CSH}, D_{LD-CSH}	Diffusivity of HD and LD C-S-H respectively
$D_{inn}, D_{int}, D_{out}$	Diffusivity of inner, intermediate and outer layer in case of multicoated sphere model
D_s	Diffusivity of solid phase in generalized effective media theory
D_0	Diffusivity in capillary pore water
E_c	total electric charge passed the sample
F	Faraday number
H()	Heaviside function
I	current passed through the sample
J	flux
J_{ss}	Steady-state flux
L	Length of sample
m	Percolation exponent
M	Molar mass of species
n	Fitting parameter representing power in different models
Q	Cumulative quantity at outlet
Q_c	Charge passed
R	Ideal gas constant
R_d	Retardation factor
r_i	Radius of i^{th} layer in case of transfer matrix method
r_{agg}	Radius of aggregates
r_c	Outer radius of the composite sphere applicable to transfer matrix method
t	Time
t_i	Components of the transfer matrix applicable to transfer matrix method
t_{itz}	Thickness of ITZ
t_{lag}	Time –lag (through-diffusion)
T	Temperature
T	Transfer matrix applicable to transfer matrix method
U	Voltage
u	Darcy velocity
w_{ea}, w_p	Weighting factors related to equivalent aggregate system and cement paste, respectively
x	Distance
z	Valency number
ϕ	Capillary porosity
ϕ_c	Threshold capillary porosity
ϕ_{pores}^i	Volume fraction of pores in i^{th} phase
ϕ_i^p	Volume fraction of i^{th} phase in cement paste
σ_e, σ_0	Effective conductivity and conductivity of pore water respectively
ρ_e, ρ_0	Effective resistivity and resistivity of pore water respectively
$\phi_{gp}^{HD-CSH}, \phi_{gp}^{LD-CSH}$	Volume fraction of gel pores in HD C-S-H and LD C-S-H respectively
$\phi_{AF}^{inn}, \phi_{CH}^{inn}$	Volume fraction of capillary pores, Aluminate phases, portlandite and C-S-H phase respectively in inner layer in case of multicoated sphere models
$\phi_{CP}^{int}, \phi_{AF}^{int}, \phi_{CH}^{int}$	Volume fraction of capillary pores, Aluminate phases, portlandite and C-S-H phase respectively in intermediate layer in case of multicoated sphere models
$\phi_{CP}^{out}, \phi_{AF}^{out}, \phi_{CH}^{out}, \phi_{CSH}^{out}$	Volume fraction of capillary pores, Aluminate phases, portlandite and C-S-H phase respectively in outer layer in case of multicoated sphere models
$\phi_{paste}, \phi_{agg}, \phi_{itz}$	Volume fraction of paste, aggregates and ITZ respectively in mortar/concrete
ϕ_{tot}	Total porosity in cement paste (gel pores + capillary pores)
$\phi_{ea}, \phi_{ea,c}$	Volume fraction and critical volume fraction of equivalent aggregate system, respectively
Ψ	electrical potential
τ	Geometric tortuosity factor
τ_a	Apparent tortuosity factor
δ	Constrictivity
θ	Water content
ε	Dielectric permittivity

1. Introduction

Chemical degradation processes of cement-based materials such as chloride-induced corrosion [1], sulphate attack [2,3], carbonation [4–6] and calcium leaching [7–10] are associated with the transport of solutes, either as ions or dissolved gases. One of the important transport mechanisms of solutes is diffusion which is driven by concentration gradients. The rate of diffusion is characterized by diffusion coefficient, commonly referred as diffusivity. Diffusivity is an important parameter for modelling processes related to contaminant transport in cementitious barriers, assessment of long-term behaviour of nuclear waste disposal systems based on cementitious engineered barriers and rebar corrosion in civil concrete structures [11]. Diffusivity is also used as a key durability parameter to define service life of concrete structures [12]. Diffusivity of a porous media at the macroscopic scale is given as [13]:

$$D_e = \frac{\theta D_0 \delta}{\tau^2} \tag{1}$$

where D_e is the diffusivity of ion/gas in porous media also known as effective diffusivity [$L^2\ T^{-1}$]; D_0 is the diffusivity of the solute in pore water [$L^2\ T^{-1}$]; θ is the volumetric water content which is equal to porosity for saturated media [−]; δ is the constrictivity factor [−] and τ is the geometric tortuosity factor [−]. The ratio (D_e/D_0) is commonly

referred to as relative diffusivity of the media [14]. Alternatively Eq. (1) can also be represented as [13]:

$$D_e = \theta D_0 \tau_a \tag{2}$$

where τ_a [−] is the apparent tortuosity factor which lumps together the effect of tortuosity and constrictivity. In case of sorption/binding of ions to solids, for example binding of chloride ions in cement-based materials, diffusivity is given as [15]:

$$D_a = \frac{D_p}{R_d} \tag{3}$$

where D_a [$L^2\,T^{-1}$] is the apparent diffusivity also accounting for retardation caused by binding/sorption, D_p [$L^2\,T^{-1}$] is the pore diffusivity ($D_p = D_0\delta/\tau^2$) and R_d [−] is the retardation factor. If no sorption of solute occurs, R_d is 1 and D_a equals D_p. It should be noted that while D_a might vary with time if sorption is non-linear, D_p remains constant. The apparent diffusivity is also commonly referred to in literature as non-steady-state diffusivity and effective diffusivity as steady-state diffusivity in case of chloride ion transport through cement-based materials [16,17]. Both constrictivity and tortuosity depend on the morphology of the media. The geometric tortuosity factor takes into account that diffusion occurs only through connected pathways. Constrictivity accounts for narrowing of pores thus restricting the diffusion of species through the pore. Constrictivity depends on the ratio of the diameter of the diffusing particle to the pore diameter. Moreover, phenomena such as anion exclusion [18], double layer effects [18,19] and influence of adsorbed layer on diffusion [20] and can be indirectly accounted for in the constrictivity. Effects of constrictivity factors on diffusivity of cement-based materials have been observed experimentally, and it has been reported by different researchers that different ions have different relative diffusivity in the same testing cement-based materials [21,22]. However, there is lack of substantial experimental data on effect of constrictivity factors in cement-based materials to establish an appropriate description of constrictivity. Hence, sometimes the relationship for constrictivity factor defined for soils has been used for cementitious materials [23].

The morphology of the cement-based materials depends on several factors such as water-to-cement (w/c) ratio, admixtures, initial composition of cement clinkers, curing conditions and degree of hydration. The morphological heterogeneities in cement-based materials can be linked with four spatial scales, viz., nano-, micro-, meso- and macro-scale. The nano-scale deals with the description of the heterogeneities associated with the calcium-silicate-hydrate (C-S-H) phase which is the main mineral phase in cement paste. It is now accepted in the cement community that there exist two types of C-S-H phases [24,25]: a low-density C-S-H phase (LD C-S-H) formed during the early stage of hydration and a high-density C-S-H (HD C-S-H) formed during the later stage of hydration. The porosity in the C-S-H matrix is referred to as gel pores. Micro-scale deals with the description of heterogeneities of the hardened cement paste (HCP). HCP morphology comprises of a wide range of solid mineral phases besides C-S-H such as portlandite (CH), aluminate phases such as ettringite (AFt), monosulphate (AFm) and hydrogarnet. HCP also contains spaces called capillary pores filled with water or air. Additionally, the matrix can also contain microcracks formed during the hardening phase. Thus, diffusion in cement paste occurs essentially through the water-filled gel pores in C-S-H and capillary pores in absence of microcracks. The meso-scale describes heterogeneities associated with the mortar/concrete and consists of aggregates, HCP and a region between cement paste and aggregates commonly referred to as interface transition zone (ITZ) which has higher porosity compared to the bulk HCP [26,27]. Furthermore, cracks and air-voids can also be present in mortar or concrete. Finally, at the macro-scale, cement-based material is treated as a homogenous material.

During the last decade, considerable efforts have been made in understanding the process of diffusion in concrete and measuring its diffusivity for which varieties of methods have been proposed. However, there is no univocal agreement on a best suited approach to measure diffusivity. Similarly, different analytical models have been developed to predict the diffusivity of cement-based materials. The increase in computational power has also enabled to compute diffusivity utilizing microstructures generated from microstructure models of HCP as input through computational homogenization which involves solving of the mass transport equation on microstructures. Different numerical approaches have been used for this purpose such as random walk [28,29], finite element [30,31], lattice Boltzmann [32] and finite difference methods [33]. Similarly, diffusivity of mortar and concrete has been determined explicitly from the meso-structure [34,35]. Hierarchical approaches wherein diffusivity computed at the micro-scale serves as input to the meso-scale have also been proposed [14,31,36,37]. However, to the authors' knowledge there is no consolidated and comprehensive overview of the existing experimental as well as modelling approaches to determine effective diffusivity of saturated cement-based materials till date. There already exist reviews on certain aspects of transport in cement-based materials such as chloride binding [38] and diffusion in unsaturated cement-based materials [39]. Fundamentals of diffusion in cement-based materials have also been discussed in [40]. Therefore the objective of this paper is directed towards fulfilling this gap. Different experimental techniques for obtaining diffusivity and issues associated with interpreting the results from these techniques have been discussed in Section 2. Section 2 also includes discussion on qualitative and quantitative trends based on compilation of dataset of measured effective diffusivity reported by different researchers, including its implications is presented. Existing analytical models to predict diffusivity have also been reviewed along with discussions on assumptions involved in these models in Section 3. Our analysis of available experimental data reveals that ITZ has only minor contribution to diffusivity and that there exists a one-to-one correspondence between mortar/concrete diffusivity and fraction of HCP in mortar/concrete. Hence, in Section 3, a comparative study and discussion only on performance of the analytical models for cement paste has been presented. The scope of this paper has been limited to diffusivity of ordinary Portland cement paste under saturated conditions. A detailed review on aspects related to determination of diffusivity directly by solving field equations on micro- and meso-structures is beyond the scope of this paper.

2. Measurement and interpretation of diffusivity in cement-based materials

2.1. Governing equations for diffusion in saturated cement-based materials

The molecular diffusion of i^{th} species through porous media can be expressed using Fick's first law which states that the diffusive flux (J [$NL^{-2}\,T^{-1}$]) is directly proportional to the concentration gradient (∇C[NL^{-2}]):

$$J^i = -D_e{}^i \nabla C^i \tag{4}$$

where C is the concentration in the aqueous phase [NL^{-3}]. Fick's first law can be used to determine diffusivity from diffusion experiment under a steady-flux condition. Fick's first law is purely phenomenological and for the case of ionic species, diffusion is more rigorously described using Nernst–Planck equation which for i^{th} ionic species is given as [41]:

$$J^i = -D_e^i \nabla C^i - D_e^i C^i \frac{z^i F}{RT} \nabla \Psi - D_e^i C^i \nabla \ln \gamma^i \tag{5}$$

z is the valence number [−]; F is the Faraday constant (96485.33289C/mol); R is the ideal gas constant (8.3145 J/mol K); T is the temperature of the liquid [K]; Ψ is the electrical potential [$ML^2T^{-2}Q^{-1}$]; and γ is the

chemical activity coefficient [−] which for low ionic strength solutions is usually computed using the Davies equation [42]. In Eq. (5), the first, second and third terms describe diffusion, electro-kinetic effects and chemical activity effects, respectively. The electrical potential in Eq. (5) is evaluated using the Poisson equation [42]:

$$\nabla^2\Psi + \frac{F}{\varepsilon}\left[\sum_i^N z_i C_i\right] = 0 \tag{6}$$

where ε [$C^2N^{-1}L^{-2}$] is the dielectric permittivity of the solution; and N is the total number of ionic species [−]. For very dilute solutions (ionic strength <0.005) the chemical activity coefficient approaches towards unity [43] supporting the simplifying assumption that $\ln\gamma \to 0$ in such case. Another simplifying assumption is that all species have the same diffusivity which implies that net transport of charge is zero. Under these assumptions second and third term of Eq. (5) can be neglected and it reduces to Eq. (4). However, the validity of these assumptions depends on the experimental conditions. Electro-kinetics effect can be of importance while interpreting ion diffusion experiments and differences in diffusivity obtained using Nernst–Planck equation and Fick's first law in some cases can amount to up to 50–100% depending on the test setups [44]. It should be noted that the setups can be designed for (chloride) ion diffusion wherein this effects can be neglected and Fick's law holds (see discussion in [44]). Similarly, Tang et al. [45] has noted that while the chemical activity effects can be neglected, the contribution from the counter ion potential due to electro-kinetic term cannot be neglected while interpreting non-steady state chloride diffusivity data.

The change in concentration in a control volume over time can be described using mass conservation in absence of chemical reactions which is known as Fick's second law as:

$$\frac{\partial \theta C^i}{\partial t} = -\nabla J^i \tag{7}$$

To account for reactive species such as chloride ions which binds with the cement matrix, and additional source/sink term has to be introduced in Eq. (7)

$$\frac{\partial \theta C^i}{\partial t} = -\nabla J^i + R^i \tag{8}$$

Where R^i denotes the source-sink term because of chemical interactions [$N^1L^{-3}T^{-1}$]. Binding of chloride in cement-based material is characterized by binding capacity, $\frac{\partial C_b}{\partial C}$ (C_b [kg/$m^3_{concrete/mortar/paste}$] and C [kg/$m^3_{solution}$] are bound and free chloride concentrations, respectively), and correspondingly, $R = -\frac{\partial C_b}{\partial t} = -\frac{\partial C_b}{\partial C}\frac{\partial C}{\partial t}$. Thus, under the assumption of constant water content with time, Eq. (8) for chloride ion diffusion can be rewritten as

$$\frac{\partial C}{\partial t} = -\frac{1}{\left(\theta + \frac{\partial C_b}{\partial C}\right)}\nabla J \tag{9}$$

For dilute solutions with no net transport of charge, Fick's first law is valid. Therefore, by substituting Eq. (4) in Eq. (9), a form equivalent to Fick's law can be derived with apparent chloride diffusivity given as:

$$D_a = \frac{D_e}{\theta\left(1 + \frac{1}{\theta}\frac{\partial C_b}{\partial C}\right)} = \frac{D_p}{R_d} \tag{10}$$

with

$$R_d = 1 + \frac{1}{\theta}\frac{\partial C_b}{\partial C} \tag{11}$$

This equation shows that the apparent chloride diffusivity (non-steady state chloride diffusivity) is dependent on binding capacity. Binding isotherm for chloride ion in cement-based materials is generally non-linear [38] and hence apparent chloride diffusivity varies with time as binding capacity intrinsically depends on concentration. However, under the simplifying assumption that binding isotherm is linear (i.e. constant D_a) so-called *erfc* type analytical solutions can be derived [46]. The governing equations described above can always be solved numerically while interpreting experimental data to obtain apparent or effective diffusion coefficients. However, depending on the test setups and boundary conditions, analytical solutions for the governing equations can be used for interpretation under certain assumptions as detailed in next section.

2.2. Measurement techniques and its application

In this study, experimental setups to determine diffusivity are classified into four categories: (i) through-diffusion based on measuring fluxes, (ii) in-diffusion based on measuring concentration profiles in the sample, (iii) electro-migration experiments, either by through- or in-diffusion, in which ion diffusion is accelerated by an electric field, and (iv) techniques in which proxy variables are used to determine diffusivity, for example, electrical resistivity techniques. A summary of the measurement techniques is given in Table 1.

2.2.1. Through-diffusion

The diffusion coefficients of a variety of diffusing species (e.g. tritiated water (HTO), ions and dissolved gases) are classically determined by the through-diffusion technique because of its simplicity, convenience and natural-like diffusion. The setup (Fig. 1a) consists of a thin sample located between two compartments. The diffusing species is injected/filled to the upstream compartment. For measuring diffusivity of dissolved gases, two gases with the same pressure are injected to the downstream and upstream compartments to balance the pressure in the two compartments which prevents advective transport. This setup usually allows measuring the diffusivity of two dissolved gases in a single experiment [47–49]. Under the concentration gradient, the diffusing species diffuses towards the downstream compartment. The concentration of diffusing species in the downstream compartment is measured regularly until steady-state flux is reached.

Fig. 1b shows a typical cumulative quantity of a diffusing species over time. When steady-state is reached, the slope becomes constant which means the diffusive flux across the sample is constant. Fick's first law (Eq. (4)) can then be applied to calculate the cumulative quantity $Q(t)$ [N] of diffusing species passed through a sample with a cross-sectional area A [L^2]:

$$Q(t) = \int_0^t -D_e A\frac{\partial C}{\partial x}dt = -D_e A\frac{\partial C}{\partial x}t \approx D_e A\frac{C_S}{L}t \tag{12}$$

where L is the length of sample [L], C is the concentration [NL^{-3}] and C_s is the concentration of diffusing species in the upstream compartment [NL^{-3}]. Note that in above equation the concentration of diffusing species in the downstream compartment (C_1) is considered to be zero as it would be negligible compared to C_s. The effective diffusivity in this case can be easily computed from the slope of $Q(t)$ curve. In case of no sorption/binding, the accessible porosity of the sample can be determined from the time-lag t_{lag} [T] (Eq. (13)), which is the intercept of the straight line with the x axis in Fig. 1b and expressed as follows [50]:

$$\theta = \frac{6D_e t_{lag}}{L^2} \tag{13}$$

Table 1
Summary of methods to measure diffusion coefficients of cement-based materials.

Technique		Through-diffusion	In-diffusion	Electro-migration	Electrical resistivity
Description/principle		• Thin sample located between two compartments; • The diffusing species is injected to the upstream compartment; • The concentration of diffusing species in the downstream compartment is measured regularly until a steady-state flux is reached.	• Based on the measurement of the concentration profile of the diffusing species inside the sample.	• Thin sample located between two electrodes; • Transport of ionic species is accelerated by an electrical potential difference; • Non-steady-state: concentration profile of ion is measured inside the sample; • Steady-state: concentration of ion in the downstream compartment is monitored until steady--state is reached.	• The electrical resistivity of the sample is measured by applying a known alternating current/voltage; • Diffusivity can be obtained from the link between resistivity and diffusion.
Conventional interpretation approach		Fick's first law	Fick's second law	Nernst–Planck equation	Nernst–Einstein equation
Pros		• Simple • Accurate • Pure diffusion	• Standardized in many codes • Possible to measure diffusivity of in situ concrete	• Relatively fast; • Standardized in many codes	• Very fast in determination of sample resistivity; • Simple setup
Cons		• Time-consuming; • Requires constant concentration gradient; • Very thin sample; • Microstructural may change due to hydration during long measurement.	• Laborious; • Less accurate in determination of profile concentration; • Still time-consuming to collect enough data points	• Issues with interpretation of results • Electro-osmotic flow and heat generation due to current; • All ions in pore solution are considered.	• Need to determine the resistivity of pore solution to calculate the effective diffusivity; • Gives only approximate diffusivity of the sample, not for specific species. • Scattered results.
Application on:	Cement	Usually for cement paste	x	x	x
	Mortar		x	x	x
	Concrete		Limited due to difficulty in sliding the sample	x	x
Obtained parameters[a]:	D_e	x		x	x
	D_a		x	x	
	θ	x		x	
Test duration		Few months	Few weeks	Few days	Instantaneous (excluding time for determination of pore solution resistivity)
Diffusing species		Dissolved gases; Ions	Ions; Radioactive elements	Ions	Not specific

[a] The obtained parameters can vary depending on the way of interpretation.

However, it has been reported that the porosity determined from time-lag is less precise than traditional porosity measurements (e.g. water saturation method) [50].

To maintain a constant concentration gradient, the gas/solution in upstream and downstream compartments is regularly refreshed. Despite this the constant gradient condition is difficult to achieve and small variations in concentration gradient at steady state can be permitted [50]. If the variations are too large, the effective diffusion coefficient can be obtained through fitting using a numerical solution of Eqs. (7) and (4) with time varying boundary conditions [47,48].

The through-diffusion technique has also been used to determine the steady-state diffusion coefficients of ions (chloride, sulphate) [51,52]. However, through-diffusion is not an optimal method to measure the steady-state diffusion coefficient for interacting (sorbing) species as it takes very long time to reach steady-state. Alternatively, electro-migration technique (see Section 2.1.3) enables to obtain the steady-state diffusion coefficient in a shorter time period. The data on diffusion of dissolved gases in saturated cement-based materials measured using through-diffusion technique is very scarce in literature and no widely-accepted standardized procedure is available so far. Knowledge of the diffusion of dissolved gases such as oxygen which is involved in the corrosion process of steel bars in reinforced concrete is important. The effective diffusion coefficients of dissolved oxygen are usually determined by through-diffusion technique in which the concentration of oxygen at downstream compartment is measured using an electrochemical method [53,54] involving cathodic consumption of the

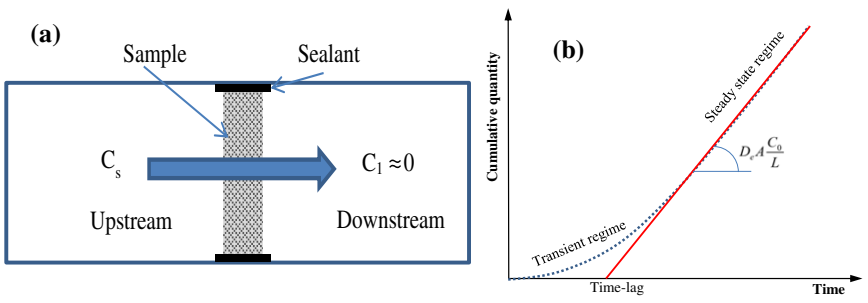

Fig. 1. (a) Through-diffusion setup (b) cumulative quantity in the upstream compartment.

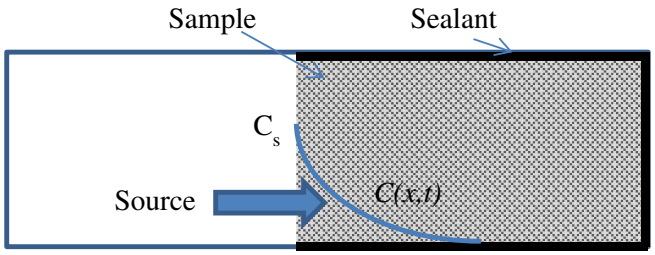

Fig. 2. Typical in-diffusion setup.

diffused oxygen and cumulative quantity is calculated using Faraday's law as [54]:

$$Q(t) = \frac{E_C}{F}\frac{M}{z} \tag{14}$$

where E_C [Q] is the total electric charge passed; F is the Faraday number (96,485 coulomb/mol); M [M^1 N^{-1}] is the molar mass of species; and z is the number of electrons transferred per molecule of species ($z = 4$ for oxygen). Recently, Phung [47,48] applied the through-diffusion technique (concentration is directly measured by gas chromatography) to measure the effective diffusion coefficients of two dissolved gases in a single experiment which can also be used for oxygen.

2.2.2. In-diffusion

Instead of waiting for a steady-state flux as in the case of through-diffusion setup, in-diffusion is a transient method, which is less time-consuming. This technique is destructive technique and only applicable on easily traceable species (chloride, radioactive elements). The technique is based on the measurement of the concentration profile of the diffusing species inside the sample by cutting the sample into small slices at a given time. Experiments are usually designed in such a way that the source concentration of the diffusing species is kept constant and the sample is long enough to consider a semi-infinite domain (see Fig. 2). The apparent diffusion coefficient is then obtained, under the assumption of a constant D_a in time and space (which implies linear binding isotherm as discussed in Section 2.1), by fitting the concentration profile with the analytical solution of Eq. (7) and (9) [55,56]:

$$C(x,t) - C_0 = (C_s - C_0)\,erfc\left(\frac{x}{2\sqrt{D_a t}}\right) \tag{15}$$

where $C(x,t)$ is concentration at depth x [L] and time t [T]; C_0 and C_s are the initial and source concentrations; respectively [NL^{-3}] and *erfc* is the complementary error function. In above equation D_a equals to D_p in case of no binding. In practice, for chloride diffusion, measurement of concentration in pore solution as a function of depth is extremely difficult. Therefore, the total chloride concentration is normally determined by profile grinding method [57]. In that case, Fick's second law is written for total concentration and equivalent forms (like Eqs. (7) and (9)) can be obtained [58], which results in an identical analytical solution as given by Eq. (15) in terms of total concentration. It is worth mentioning that the apparent chloride diffusion coefficient for cementitious materials derived using Eq. (15) decreases with the duration of measurement [59] due to continuous hydration and non-linear binding. Moreover, the diffusion coefficient obtained from Eq. (15) is not the instantaneous diffusion coefficient at a given exposure time but reflects a kind of an average effect at that time.

Chloride diffusion coefficients are commonly determined using long-term immersion tests based on the in-diffusion method which have been standardized in ASTM C1556-04 [60] and Nordtest NT Build 443 [57] and recently in European Standard EN 12390-11 – part 11 [61]. As diffusion is the main transport mechanism in these tests, the exposure duration is quite long in order to collect enough experimental data, even with concentrated chloride concentration (165 g NaCl per litre) for Nordtest NT Build 443, the required exposure duration is still 35 days. The diffusivity obtained from long-term immersion tests is frequently based on Fick's second law which does not take into account ion-ion interactions and binding effects. However, the diffusivity obtained from Nordtest NT Build 443 is referred as the "effective" diffusivity which should actually be the "apparent" diffusivity.

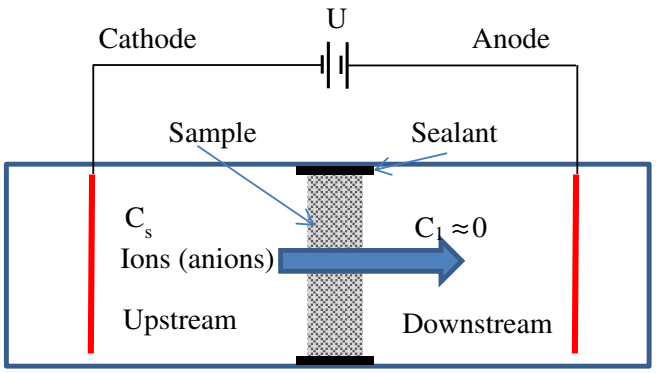

Fig. 3. Electro-migration diffusion setup.

The mentioned assumptions for interpretation of long-term immersion tests could lead to controversial results, for example, the diffusivity of chloride in sodium chloride solution is smaller than in potassium chloride because the diffusivity of potassium is higher than that of sodium [62] resulting in a larger influence of electro-kinetic effect on chloride diffusion. Furthermore, chloride diffusivities obtained from long-term immersion tests are higher than electro-migration tests despite the good correlation between two obtained diffusivities [17,63]. Therefore, the use of Nernst-Planck equation instead of Fick's law is recommended to interpret data from long-term immersion tests to account for transport of charge [45].

Besides chloride ions, diffusion of sulphate ions is also a relevant because sulphate attack is an important durability problem in coastal concrete structures. The diffusion coefficient of sulphate ions is normally measured by an in-diffusion method in which the sample is placed in a sodium sulphate solution (5%) [64]. A similar test protocol for chloride can also be applied for the determination of sulphate diffusion coefficient [65,66].

2.2.3. Electro-migration

Electro-migration tests have been developed to accelerate the ionic transport by applying an electrical field. The setup consists of a thin sample located between two electrodes immersed in electrolyte solutions (see Fig. 3). The ionic species for which diffusivity has to be measured is added to the upstream compartment. A constant electrical potential difference is applied across the sample. In steady-state migration tests, the evolution of the concentration of a given ionic species in the downstream compartment is monitored until steady state is reached. For non-steady-state migration tests, the concentration profile of the ionic species within the sample is measured after a given period. The interpretation of experimental data to obtain diffusion coefficient is carried out using Nernst-Planck equation (Eq. (5)). Under assumptions of a constant D_a, constant electrical field (i.e. $\nabla\Psi = \Delta\Psi/L$), negligible contribution of electro-kinetic term compared to electrical field, and semi-infinite domain, the analytical solution for Nernst-Planck equation can be obtained and the concentration profile (for non-steady-state tests) is given as [67]:

$$C = \frac{C_s}{2}\left[e^{ax}erfc\left(\frac{x + aD_a t}{2\sqrt{D_a t}}\right) + erfc\left(\frac{x - aD_a t}{2\sqrt{D_a t}}\right)\right] \tag{16}$$

where $a = \frac{zF\Delta\Psi}{RTL}$; C_s is the source (boundary) concentration [NL^{-3}]; L is the length of sample [L] and $\Delta\Psi$ is the potential difference

$[ML^2T^{-2}Q^{-1}]$. The apparent diffusion coefficient can be obtained by fitting the concentration profile using Eq. (16) (as in the case of in-diffusion technique). Note that the apparent diffusion coefficient obtained in this case (under assumption of a constant electrical field) may be higher than one derived from conventional diffusion experiments (through-diffusion) because ionic concentration profiles are overestimated as pointed out by Samson el al. [42].

For steady state (i.e. constant flux in the domain) under the assumptions that electro-migration is the dominant transport process (i.e. the first term and last term of the right-hand side of Eq. (5) are neglected), the electrical filed is constant (even this assumption may not be verified [42]), and upstream concentration is much higher than downstream concentration, the effective diffusion coefficient can be computed as follow (similar to through-diffusion):

$$D_e = \frac{J_{SS} RTL}{zFC_s \Delta\Psi} \tag{17}$$

The steady-state flux J_{SS} $[NL^{-2}T^{-1}]$ can be calculated from the concentration evolution in the downstream compartment.

Electro-migration tests offer a possibility to significantly shorten the measurement time for ionic species [16,67–69]. For cement-based materials, the most commonly investigated ion is chloride, because of the extent of reinforcement corrosion damage due to de-icing and exposure to marine environment. Electro-migration test for chloride has been standardized in many national standard procedures. In Nordtest NT 355 [70], the steady-state migration test is used to determine the effective diffusivity by applying a constant direct voltage U of minimum 12 V during minimum exposure duration of 7 days. The Eq. (17) is then used to interpret the experimental data. Nordtest NT Build 492 [71], on other hand, proposes use of a non-steady-state chloride migration test in which in range of 10–60 V (typically experiments are carried out at high voltage of 30 V) is applied on samples in 10–96 h depending on the concrete quality. The apparent diffusivity is then calculated using Eq. (18) which is a simplified form of Eq. (16) under the assumptions that the penetration depth x_d [L] (measured using colorimetric method) is larger than $\alpha D_a t$ and the electrical field is large enough. These assumptions are indeed acceptable for this setup.

$$D_a = \frac{RTL}{zF\Delta\Psi} \frac{x_d - \alpha\sqrt{x_d}}{t} \tag{18}$$

where

$$\alpha = 2\sqrt{\frac{RTL}{zF\Delta\Psi}} erf^{-1}\left(1 - \frac{2C_d}{C_s}\right) \tag{19}$$

where C_d $[NL^{-3}]$ is the chloride concentration at which the colour changes when measuring x_d ($C_d \approx 0.07$ N for OPC concrete). Note that $\Delta\Psi = U - 2$ taking into account the drop of 2 V between the interface of the electrode and the electrolyte. The non-steady-state diffusion coefficients obtained from the mentioned electro-migration methods are reported to be about one order of magnitude higher than the steady-state diffusion coefficients [72]. This is due to the fact that the effective diffusible area (porosity) is less than the apparent cross-sectional area of the sample, while the binding effect counteracts this difference (see Eq. (10)) [73]. The heat generation during electro-migration tests also strongly contributes to deviation of test results [74,75].

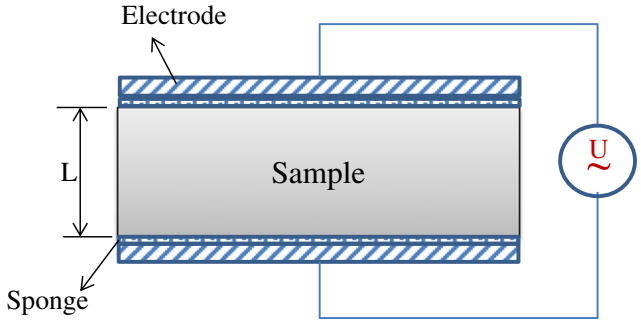

Fig. 4. Typical electrical resistivity setup.

ASTM C1202-97 [76] also involves in measuring the electrical currents at different experimental time under a voltage of 60 V applied on the sample immersed in a sodium chloride solution at one end, and in a sodium hydroxide solution at the other end, in duration of 6 h. The electrical currents are then used to calculate the charge passed through the sample, which is clamed as an indicator for chloride resistance.

$$Q_c = 900(I_0 + 2I_{30} + \ldots + 2I_{300} + I_{360}) \tag{20}$$

where Q_c [coulombs] is the charge passed; I_0 is the current [amperes] immediately after voltage is applied, and I_t is the current [amperes] at t minutes after voltage is applied. The concrete is considered having a high chloride resistance if Q_c is smaller than 100 coulombs and a high chloride penetration if Q_c is larger than 4000 coulombs. However this method may not correctly reflect the chloride diffusion through the sample because it does not take into account the effect of presence of other ions in pore solution which strongly influences the measured electrical currents. This method is in fact, as also stated in the standard ASTM C1202-97, only applicable to types of concrete which have a good correlation between the charge passed and the diffusion coefficient determined by long-term migration tests.

2.2.4. Electrical resistivity

The effective diffusivity can be alternatively obtained by exploiting the analogy between electrical conductivity and diffusivity in a porous material. Based on the Nernst–Einstein equation [77], diffusion, electrical conductivity and resistivity are linked as:

$$\frac{D_e}{D_0} = \frac{\sigma_e}{\sigma_0} = \frac{\rho_0}{\rho_e} \tag{21}$$

where σ_e and σ_0 $[M^{-1}L^{-3}T^3I^{-2}]$ are the electrical conductivity of the sample and of pore solution, respectively and ρ_e and $\rho_0[M^1L^2T^3I^{-2}]$ are the electrical resistivity of the sample and the pore solution, respectively. The electrical resistivity of the sample is measured by applying a known alternating current/voltage (Fig. 4). The resistivity of the sample can be then determined as:

$$\rho_e = \frac{\Delta\Psi}{I}\frac{A}{L} \tag{22}$$

where Ψ and I [I] are the electrical potential and current passed through the sample, respectively and A $[L^2]$ and L [L] are the cross sectional area and length of the sample, respectively. To estimate diffusivity, determination of the pore solution resistivity is also required which is not straightforward. To determine pore solution resistivity, pore solution has to be extracted under extremely high pressure (up to 400 MPa). Alternatively, electrical resistivity can also be estimated if the pore water composition of cement paste is known [78]. Another approach to eliminate this problem is to replace the pore solution by a solution with known resistivity [79], which might increase experimental duration and also alter resistivity of cement matrix due to its interaction with this solution. Alternatively, an empirical relation can be established between electrical resistivity and diffusivity which can be then used to interpret diffusivity from electrical resistivity [73,80,81]. Electrical resistivity is commonly utilized for concrete quality control as it is fast and relatively simple to measure [82,83]. Spragg et al. [84] have analysed in detail different factors affecting electrical resistivity measurements. They reported that several key parameters such as setup, temperature, sample storage and conditioning, frequency of current at

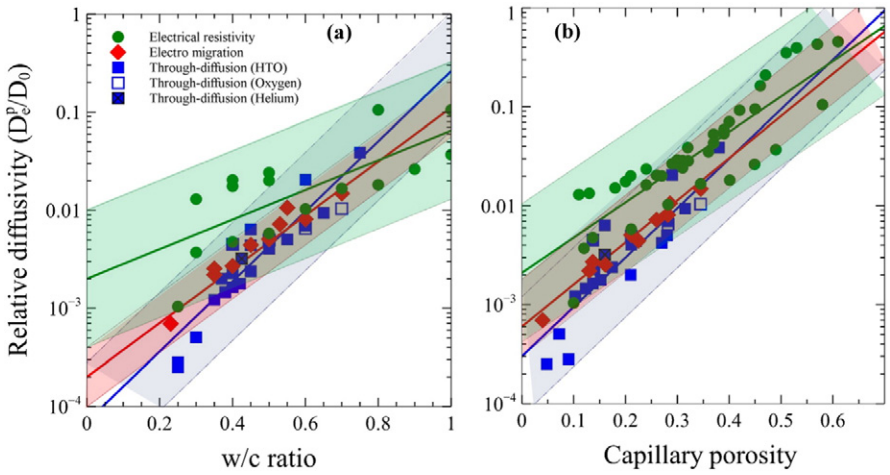

Fig. 5. Relative diffusivity vs. w/c ratio (a) and capillary porosity (b): data is fitted to an exponential relationship of form given in Table 2 (thick solid lines) for each experimental technique; shaded regions represent the region in which all data fall around the exponential relation with a factor 5-, 2- and 4- bounds for electrical resistivity, electro-migration and through-diffusion, respectively.

which measurements are carried out, and the pore water solution may result in large variations of the relative diffusivity obtained by the electrical resistivity measurements.

2.3. Comparison of relative diffusivities obtained by different techniques

2.3.1. Hardened cement pastes

Diffusivity data for ordinary Portland cement paste (without supplementary materials) as published by different researchers using different techniques have been compiled and compared in this section. The data includes measurements carried out using (i) through-diffusion experiments for HTO [53,85–89] and dissolved gases such as helium [48] and oxygen [53,90], (ii) electrical resistivity [91–94] and (iii) electro-migration for steady-state chloride ion diffusivity [95–97]. The non-steady-state chloride diffusion coefficients were not included in this comparison as the apparent diffusivity measured by these tests, as discussed in Sections 2.1 and 2.2, varies depending on duration of measurements due to binding of chloride ions with cement matrix. For the readers who are interested in comparison of non-steady-state chloride diffusivity obtained from different methods, we refer to the work of Tang et al. [73].

The relationship between for HCP relative diffusivity (D_e^p/D_0) (where the superscript p refers to HCP) and w/c ratio and capillary porosity for the collected data is shown in Fig. 5. Note that for data where the capillary porosity is not reported, Power's model [98] in which w/c ratio and hydration degree are input parameters is used to estimate the capillary porosity. The degree of hydration needed in the Power's model is obtained from the relation proposed by Bejaoui and Bary [99], which gives maximum degree of hydration. Increase in relative diffusivity with respect to w/c ratio and capillary porosity is consistent for all reported data. The relation of the relative diffusivity with w/c ratio shows more scatter than with capillary porosity. This is because of the fact that at a given w/c ratio, the degree of hydration achieved might vary for the reported data, which in turn can result in different porosities. Regardless of the use of different experimental techniques and studies, all reported data is well fitted to the exponential relationship correlating the relative diffusivity with w/c ratio or capillary porosity. Data for different experimental techniques have been grouped together and separately fitted. The data obtained by electrical resistivity show most scatter (fitted within factor 5-bounds -area in between the line drawn by multiplying and dividing five with the best fit value or line of equality), whereas electro-migration data provide the best fit (within

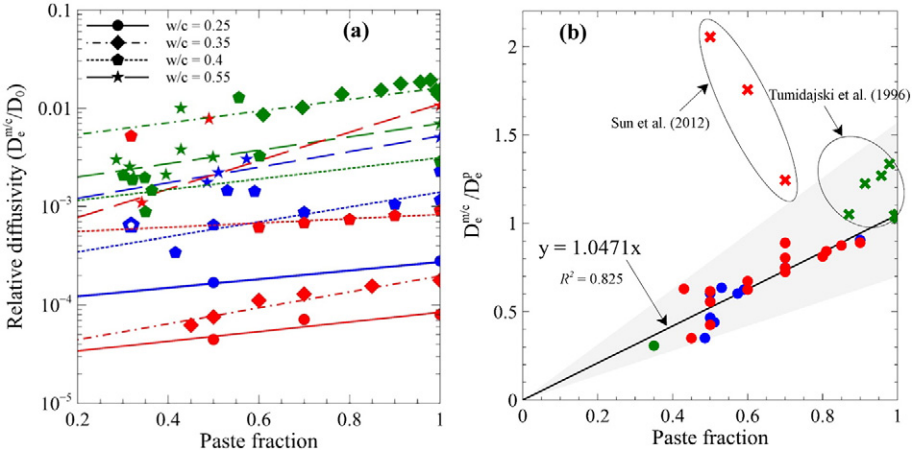

Fig. 6. (a) - Relationship between the relative diffusivity, paste fraction and w/c ratio of mortar/concrete: continuous lines fitted to exponential relationship of form given in Table 2, red = electro migration, blue = through-diffusion, green = electrical resistivity, hollow pentagon represents the diffusivity of chloride using through-diffusion; and ratio between diffusivity of mortar/concrete and bulk paste vs. paste fraction; (b) - Ratio between the effective diffusivity of mortar/concrete and cement paste at the same w/c ratio versus the paste volume fraction: linear line is fitted with data points, red = electro migration, blue = through-diffusion, green = electrical resistivity, data in cross not included in regression, shaded region represents the region in which all data fall around the linear relation with a factor 2.

factor 2-bounds). As seen in Fig. 5 the relative diffusivity obtained from electrical resistivity generally shows a tendency for higher values compared to through-diffusion and electro-migration techniques. These differences can be up to an order in magnitude for low w/c ratio or capillary porosity and diminishes with the increase of w/c ratio or capillary porosity, in particular, when w/c ratio is larger than 0.65 this differences are minimal. Because different measurement techniques do not measure the contribution of different pore types to the transport process in the same way, measured diffusivities may vary between different techniques. We believe that for electrical resistivity, the current can be transmitted through a wide range of pores including capillary, gel and inter-layer pores. On the other hand, the contribution of small gel pores in C-S-H to the diffusion process might be negligible for through-diffusion and electro-migration. Therefore, at low w/c ratio at which C-S-H is the dominant phase for transport, small gel pores might be hardly accessible for species, whereas it can still transmit current.

2.3.2. Mortar and concrete

Fig. 6a presents the relationship between the relative diffusivity of OPC mortar/concrete (without supplementary materials) at different w/c ratios and paste (in mortar/concrete) fraction. Data was collected from measurements using electrical resistivity [91,100–108], through-diffusion [51,85,87,109,110] and chloride steady-state diffusivity determined by electro-migration [68,69,97,111–113]. Note that for the studies in which the aggregate fraction was reported in mass, volume fractions were calculated with assumed bulk densities of aggregate and mortar/concrete as 2.35 and 2.65 g/cm^3, respectively. For electrical resistivity measurements of [101–106,108], electrical resistivity/conductivity of the pore solution is not reported and therefore the pore solution resistivity/conductivity was calculated analytically based on the cement compositions, w/c ratio and hydration degree (assumed 90%) [78,114].

It is obvious from Fig. 6a that the relative diffusivity increases with increasing paste volume fraction for all w/c ratios and measurement techniques. The porosity of the aggregate phase is very low compared to the porosity of the bulk paste. Therefore, higher paste volumes will generally increase the porosity of mortar/concrete, which results in a higher diffusivity. Similar to cement paste, the relative diffusivity of mortar/concrete obtained by electrical resistivity is higher compared to the other methods. The results from through-diffusion and electro-migration are quite similar. Nevertheless, at low w/c ratio (0.25), the diffusivity obtained by through-diffusion is higher than one by electro-migration. Similar observation has been made by Castellote et al. [51]. This might be due to the difference between penetration mechanisms in electro-migration tests (e.g. counter-convection, ion-aggregations) and in through/in-diffusion tests. Moreover, at very low w/c ratio, ions (chloride) might diffuse slower due to higher surface charge effect as reported by Yu et al. [54]. An increase of w/c ratio results in an increase in diffusivity of mortar/concrete in most cases, except for data of Tumidajski et al. [91] for w/c ratio of 0.35 using electrical resistivity. The scatter in data from electrical resistivity for mortar/concrete is attributed to the same reasons as mentioned previously for the cement paste.

In Fig. 6b, the ratio ($D_e^{m/c}/D_e^p$) between the effective diffusivity of mortar/concrete and cement paste at same w/c ratio is plotted versus the paste volume fraction in mortar/concrete. In general, $D_e^{m/c}/D_e^p$ increases with increasing paste fraction except for the results of Sun et al. [115] and some data points reported by Tumidajski et al. [91]. However, Tumidajski et al. has concluded that the diffusivity increases in mortar with increasing paste fraction and only some measurements at very low sand fraction, give slight lower diffusivities compared to cement paste, which can be attributed to inaccuracies in measurements. Sun. et al. attributed the increase of diffusivity with increasing aggregate fraction to the significantly higher diffusivity of ITZ. However, many researchers have argued that the influence of ITZ on the diffusivity is not significant [111,116,117] compared to the increase of tortuosity and decrease of porosity due to the presence of aggregate in mortar/concrete. Theoretically, when both ITZ and capillary pores are percolated, they can act as parallel pathways for transport and the effective diffusivity of mortar/concrete ($D_e^{m/c}$) can be approximately expressed as:

$$D_e^{m/c} \simeq \phi_{paste} D_e^p + \phi_{agg} D_e^{agg} + \phi_{itz} D_e^{itz} \tag{23}$$

where ϕ_{paste}, ϕ_{agg} and $\phi_{itz}$are the volume fractions and D_e^p, $D_e^{agg}$and D_e^{itz} diffusivity [L^2 T^{-1}] of mortar/concrete, paste, aggregate, and ITZ, respectively. Because the diffusivity of aggregate is nearly zero, the second term in Eq. (23) can be considered as zero. Furthermore, the slope of the regression line in Fig. 6b is nearly one, which gives following relation:

$$D_e^{m/c} \simeq \phi_{paste} D_e^p \tag{24}$$

Thus, by comparing Eqs. (23) and (24), it appears that ITZ has limited influence on the diffusivity of mortar/concrete.

3. Models to determine effective diffusivity

3.1. Effective diffusivity models for cement paste

In this section, different models to predict diffusion coefficients of cement paste are reviewed. These models typically use parameters such as porosity, w/c ratio and volume fractions of different phases in cement paste to predict diffusivity. We classify these models in this study as empirical approaches, relationships derived from numerical models and analytical relationships, the latter based on effective media theories. For the latter, a further distinction is made between models considering a simplified morphology of cement paste and models taking into account detailed morphological characteristics of hardened cement paste. These relationships are summarized in Table 2.

Empirical relationships relate the effective diffusivity with variables such as porosity and w/c ratio by fitting with experimental data. These relationships do not directly account for the morphology and connectivity of the pore structure; these factors are lumped phenomenologically in the fitting coefficients. Some of these relationship have been directly adapted from soil science. For instance, Archie's power relationship [128] was originally proposed for rocks and sand and has been adapted for cement paste. Archie's relationship was first expressed in terms of (total) porosity. However, it is usually assumed that capillary pores are the major diffusive pathway in cementitious materials. Hence, some authors [14,97] express the Archie's relationship in terms of capillary porosity. Moreover, porosity for hardened cement paste is often determined by Mercury Intrusion Porosimetry (MIP), which covers mainly the capillary pore range (2.5 nm to 100 μm) [129]. Hence, in this paper all empirical relationships have been expressed in terms of capillary porosity. Applicability of Archie's relationship to cementitious materials has been argued by some authors especially when the capillary pores are not percolated [14,21,130]. Moreover, the fitting parameters for Archie's relationship obtained in different studies vary substantially as shown in Table 3. Despite these limitations, the Archie's relationship is often used to simulate reactive transport processes in cement paste [131,132]. To alleviate the inability of Archie's relationship to account for the percolation threshold, Winsauer et al. [118] proposed to set the diffusivity to zero when the porosity is smaller than a certain threshold porosity (ϕ_c). For cement paste, the fitting parameters for this relationship have been obtained by Van Der Lee et al. [133]. The effective diffusivity can also be expressed as an exponential function of porosity instead of a power law [21,87,119]. The exponential function is also used to describe the relationship between w/c ratio and effective diffusivity [120].

Garboczi and Bentz [14] established a relationship between relative diffusivity and capillary porosity based on numerical computation

Table 2
Summary of effective diffusivity models for cement paste.

Model/references	Mathematical expressions	Fitting parameters
Empirical relationships		
Archie's relationship	$\frac{D_e^p}{D_0} = A\phi^n$	A, n
Modified Archie's relationship [118]	$\frac{D_e^p}{D_0} = A(\phi-\phi_c)^n, \forall\phi>\phi_c$ $\frac{D_e^p}{D_0} = 0, \forall\phi\le\phi_c$	A, n, ϕ_c
Exponential form [21,119]	$\frac{D_e^p}{D_0} = A\, e^{n\phi}$	A, n
Exponential form with respect to water cement ratio [120]	$\frac{D_e^p}{D_0} = A\, e^{n\,(w/c)}$	A, n
Relationships derived from numerical models		
NIST model [14]	$\frac{D_e^p}{D_0} = A_1 H(\phi-\phi_c)(\phi-\phi_c)^2 + A_2\phi^2 + A_3$	A_1, A_2, A_3 and ϕ_c
Effective media theories		
Differential effective media [121]	$\frac{D_e^p}{D_0} = \phi^{1.5}$	Free water diffusion should be taken an order of magnitude lower to apply this model to cement paste [121].
Generalized self-consistent scheme [97]	$\frac{D_e^p}{D_0} = \left(m_\phi + \sqrt{m_\phi^2 + \frac{\phi_c}{1-\phi_c}\left(\frac{D_{CSH}}{D_0}\right)^{\frac{1}{n}}}\right)^n$ $m_\phi = \frac{1}{2}\left[\left(\frac{D_{CSH}}{D_0}\right)^{\frac{1}{n}} + \frac{\phi}{1-\phi_c}\left(1-\left(\frac{D_{CSH}}{D_0}\right)^{\frac{1}{n}}\right) - \frac{\phi_c}{1-\phi_c}\right]$	D_s, n, ϕ_c
Bejaoui and Bary [99][a]	Uses different set of series parallel configurations as shown in Fig. 7. The tortuosity of capillary pores is computed through $\tau_a = 0.0067e^{5\phi}$ The tortuosity of LD C-S-H, HD C-S-H and mixed fraction of LD C-S-H and capillary porosity is computed using effective media theory for single coated sphere, which can be written as $\tau_a^i = \phi_{pores}^i - \left(\frac{\phi_{pores}^i(1-\phi_{pores}^i)}{3-\phi_{pores}^i}\right)$ i∈[LD CSH, HD CSH, LD CSH + HDCSH]	D_{LD-CSH}, D_{HD-CSH}
Bary and Bejaoui [122][a]	$D_{e,n} = D_n + \left(1-\frac{\phi_n}{\sum_{i=1}^n \phi_i}\right)\left[\frac{1}{D_{e,n-1}-D_n} + \frac{1}{3D_n}\frac{\phi_n}{\sum_{i=1}^n \phi_i}\right]^{-1}$ $D_{inn} = 2D_{HD-CSH}\left(\frac{1-\phi_{AF}^{inn}-\phi_{CH}^{inn}}{2+\phi_{AF}^{inn}+\phi_{CH}^{inn}}\right)$ Under the assumption $D_{CSH}^{out}/D_0 \approx 0$ $D_{int} = 2D_{LD-CSH}\left(\frac{1+2\phi_{CP}^{int}-\phi_{AF}^{int}-\phi_{CH}^{int}}{1-\phi_{CP}^{int}+0.5(\phi_{AF}^{int}+\phi_{CH}^{int})}\right)$ $D_{out} = D_{LD-CSH}\left(\frac{1-\frac{3}{2}(\phi_{AF}^{out}+\phi_{CH}^{out})}{1-3\phi_{CP}^{out}}\right)$	D_{LD-CSH}, D_{HD-CSH}
Stora et al. [123][a]	$D_e^p = 2D_{out}\left(\frac{3}{2+\phi_{UC}-2\phi_{inn}\beta_{inn}^{out}} - 1\right)$ $\beta_{inn}^{out} = \frac{D_{inn}-D_{out}}{D_{inn}+2D_{out}}$ $D_{inn} = 2D_{HD-CSH}\left(\frac{1-\phi_{AF}^{inn}-\phi_{CH}^{inn}}{2+\phi_{AF}^{inn}+\phi_{CH}^{inn}}\right)$ $D_{out} = 2D_{LD-CSH}\left(\frac{1+2\phi_{CP}^{out}\beta_{cp}^{LD-CSH}-\phi_{AF}^{out}-\phi_{CH}^{out}}{2-\phi_{CP}^{out}\beta_{cp}^{LD-CSH}+\phi_{AF}^{out}+\phi_{CH}^{out}}\right)$ $\beta_{cp}^{LD-CSH} = \frac{D_{cp}-D_{LD-CSH}}{D_{cp}+2D_{LD-CSH}}$ $D_i = D_{gp}\left[\frac{-1+(f_{gp}^i+\phi_{gp}^i)+\lvert 1-(f_{gp}^i+\phi_{gp}^i)\rvert}{1+(2f_{gp}^i-\phi_{gp}^i)}\right]$ i∈[LD−CSH, HD−CSH]	f_{gp}^{LD-CSH}, f_{gp}^{HD-CSH}, ϕ_{gp}^{HD-CSH}
Dridi [124][a]	$D_{e,n} = D_n + \left(1-\frac{\phi_n}{\sum_{i=1}^n \phi_i^p}\right)\left[\frac{1}{D_{e,n-1}-D_n} + \frac{1}{3D_n}\frac{\phi_n}{\sum_{i=1}^n \phi_i}\right]^{-1}$ $D_{inn} = 2D_{HD-CSH}\left(\frac{1-\phi_{AF}^{inn}-\phi_{CH}^{inn}}{2+\phi_{AF}^{inn}+\phi_{CH}^{inn}}\right)$ $D_{out} = 2D_{LD-CSH}\left(\frac{1+2\phi_{CP}^{out}-\phi_{AF}^{out}-\phi_{CH}^{out}}{1-\phi_{CP}^{out}+\phi_{AF}^{int}+\phi_{CH}^{int}}\right)$ if $\phi_{cp}^{out}<\phi_c$ $\sum_i \frac{\phi_i^{out}}{\phi_{CP}^{out}+\phi_{AF}^{out}+\phi_{CH}^{out}+\phi_{CSH}^{out}}\frac{D_i-D_{out}}{D_i+2D_{out}} = 0$ if $\phi_{cp}^{out}>\phi_c$ i∈[CP, CH, CSH_{out}, AF]	D_{HD-CSH}, D_{LD-CSH}
Liu 2009[b] [125]	$D_{LD-CSH} = \phi_{gp}^{HD-CSH1.5} D_{gp}$, $D_{HD-CSH} = \phi_{gp}^{LD-CSH1.5} D_{gp}$ $\frac{D_{CSH}-D_{LD-CSH}}{D_{CSH}+2D_{LD-CSH}} = \sum_i \phi_i^{out}\left[\frac{D_j-D_{LD-CSH}}{D_j+2D_{LD-CSH}}\right]$ i∈[CP, HD−CSH] $\sum_i \phi_i^p \frac{D_i-D_e^p}{D_i+2D_e^p} = 0$ i∈[CP, CH, AF, UC, CSH]	D_{gp} porosity of LD and HD CSH was taken as 0.37 and 0.24

[a] Volume fractions of different phases are determined using Tennis and Jennings hydration model [126].
[b] The volume fractions of different phases were determined using hydration model proposed by Bernard et al. (2003) [127].

of diffusivity from virtual cement paste microstructure. Numerical computation of diffusivity using virtual microstructures allows for distinguishing contributions of different phases, namely, C-S-H and capillary pores, to diffusion. The mathematical expression of this relationship is given in Table 2. The first term in their relationship represents the contribution of the percolating fraction of the capillary pores. The second term represents the contribution of non-percolating capillary pores and the C-S-H phase. The last term is the contribution of C-S-H when capillary porosity is zero. Through numerical simulations on virtual microstructure of hydrating C_3S paste, they determined the values for coefficients A_1, A_2 and A_3 as 1.8, 0.07 and 0.001, respectively. The threshold porosity ϕ_c was determined to be 0.18. For cement paste, Bentz et al. [134] determined the coefficients A_1, A_2 and A_3 as 1.7, 0.03, and 0.0004 respectively. The threshold porosity for cement paste was determined as 0.2. The threshold porosity computed from

Table 3
Values of coefficients and power for Archie's relationship as derived by different authors.

Reference	A	n
Tumidajski et al. [91]	1.89	2.55
Tumidajski et al. [91] using data of Christensen et al. [94]	0.14	4.8
Tumidajski et al. [91] using data of Taffinder and Batchelor [93]	7.71	3.32
Yamaguchi et al. [88]	0.18	0.94

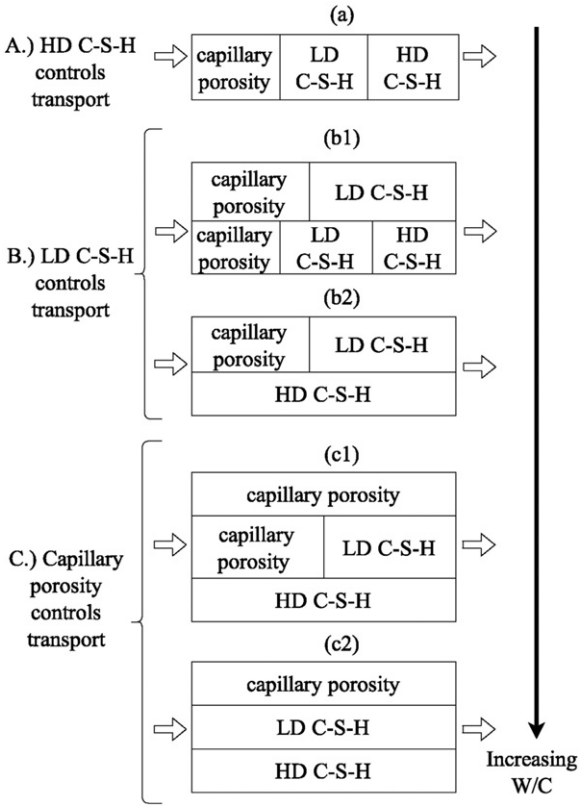

Fig. 7. Simplified morphological representations of HCP in the model of Bejaoui and Bary [99] to predict effective diffusivity.

the virtual microstructure of cement paste has been found to be independent of w/c ratio. However, it strongly depends on the resolution of the microstructure and the used microstructure model [135–137]; hence the percolation threshold can be considered as an additional adjustable parameter. Furthermore, many models discussed later in this paper use the percolation threshold value reported by Garboczi and Bentz [14]. The percolation threshold is therefore considered as an additional adjustable parameter for all the models in this paper.

The models discussed so far are fitted mathematical models to either experimental or numerical data without directly considering the morphology of HCP in deriving this relationship. Series of models have conceptualized the morphology into simple geometrical configurations for which analytical solution or theoretical models can be devised. These theories are known as effective media theory. The simplest geometrical configuration is arranging different phases of the multiphase material such as cement paste in series or parallel. Bejaoui and Bary [99] presented a set of series/parallel configurations to predict diffusivity of the cement paste as shown in Fig. 7. In their approach, percolating diffusive phases are placed in parallel whereas non-percolating phases are placed in series. The degree of percolation was computed based on volume fraction of percolating phase. They assumed that percolation of a phase starts once its volume fraction is 15% and becomes fully percolated at 25% volume fraction; in between, the degree of percolating fraction increases linearly. This function for degree of percolation is inspired from the analysis using CEMHYD3D reported by Bentz et al. [138]. The exponential law is used to calculate the tortuosity of the capillary pores, whereas the tortuosity of LD C-S-H, HD C-S-H and mixed LD C-S-H - capillary pores were taken into account using the effective media theory for single coated spheres [139]. Phase fractions were computed from the Tennis and Jennings hydration model [126] and porosities of LD and HD C-S-H were taken as 20% and 31% respectively (based on [140]). They determined the HTO diffusion coefficient of LD C-S-H and HD C-S-H as 9×10^{-12} m^2/s and 1×10^{-12} m^2/s, respectively, by fitting experimental data.

Another set of configurations for which theoretical models exist are well-defined inclusions (such as spheres, cylinders, ellipsoids) distributed randomly throughout a matrix material. The most commonly used theoretical models for such configurations are the Generalized Maxwell approximation (which is analogous to the Mori-Tanaka scheme used for elastic modulus [139]), the self-consistent scheme (and its variants, also referred to as effective media approximation [141]) and the differential effective media scheme. These models differ in the underlying assumptions used to derive the effective diffusivity. To understand the underlying assumptions, consider a composite medium of two phases. In the generalized Maxwell approximation, one phase is considered as inclusions in the other phase in an infinite domain with the same shape as the inclusion, so that a constant gradient can be assumed inside the domain. The inclusions are considered to be well separated so that they do not interact with each other. With this assumption, the analytical solution for a single inclusion can be directly applied to obtain the effective media of the composite. The applicability of generalized Maxwell approximation is limited to dilute systems with small volume fractions of the inclusions. In the self-consistent scheme, the phases are considered as inclusions in a matrix with a diffusivity equivalent to that of the effective diffusivity of the composite. It is further ensured that the local perturbations in a concentration field caused by these inclusions on average cancel out. The self-consistent scheme treats all phases of a heterogeneous medium in the same way and hence allows accounting for the effect of percolation of one phase on another phase. However, when properties of different phases vary substantially, the self-consistent approximation fails [139]. In the differential effective media scheme, one phase is taken as the matrix and another phase is added incrementally such that the added phase is always in the dilute limit with respect to current effective media. This assumption leads to a differential equation integration of which gives the effective diffusivity of the composite. The differential effective media scheme ensures that the initial matrix always remains connected. This in turn allows the differential effective media scheme to recover Archie's law [142]. Formulas for these effective media theories for two-phase composites with spherical inclusions are given in Table 4. The formula for generalized Maxwell scheme is explicit, whereas self-consistent and differential effective media schemes have implicit formula. For a detailed description of these schemes readers are referred to [139,143].

Several cement paste models have been proposed wherein cement paste has been conceptualized to be composed of inclusions in a matrix material. Pivonka et al. [121] conceptualized cement as non-diffusive spherical inclusions in a matrix consisting of capillary pore phase. Their predicted values using the differential scheme were one order of magnitude larger than values from steady-state chloride diffusivity

Table 4
Formulas for different effective media theories for a composite made of two phases for details see [139,143].

Effective media theory	Assumptions	Formulae
Generalized Maxwell's approximation	Phase 2 are inclusions in matrix of phase 1	$\frac{D_e-D_1}{D_e+2D_1}=\phi_2\left[\frac{D_2-D_1}{D_2+2D_1}\right]$
Self-consistent scheme	Phase 2 and phase 1 are inclusions in matrix of equivalent homogenous media.	$\phi_1\frac{D_1-D_e}{D_1+2D_e}+\phi_2\frac{D_2-D_e}{D_2+2D_e}=0$
Differential effective media scheme	Phase 1 is taken as matrix and phase 2 is added incrementally such that the volume fraction added is always in the dilute limit with respect to current effective media.	$\left(\frac{D_2-D_e}{D_2-D_1}\right)\left(\frac{D_1}{D_e}\right)^{\frac{1}{3}}=1-\phi_2$

measured using electro-migration techniques. They proposed that the diffusivity in the pore solution of cement paste should be ten times lower than that in pure water due to the higher viscosity of the pore solution because of restructuring of water molecules along the charged pore surfaces. With a ten times lower pore solution diffusivity, the differential approximation reduces to Archie's law with values of 0.1 and 1.5 for A and n (Table 2), respectively. Christensen et al. [94] has shown that, the differential effective media scheme provides good correlation with electrical resistivity measurements only at the early stages of hydration when capillary porosities are larger than 50%.

Oh and Jang [97] applied the generalized effective media approximation to predict effective diffusivity of cement paste. They considered cement paste as inclusions of capillary pores and diffusive solids (C-S-H) in an equivalent homogenous matrix. According to their model, diffusion in cement paste with a capillary porosity less than the threshold capillary porosity of 17% occurs through the diffusive solids. The value of the solid phase was determined as 2.0×10^{-4} by fitting with experimental data. The relationship derived from the generalized effective media theory takes a similar form as that of modified Archie's relationship proposed by Winsauer et al. [118] when diffusivity of the solid phase is zero. Therefore, modified Archie's law can also be viewed as a specific case of the generalized effective media theory.

In above discussed models morphology of cement paste has been drastically simplified. Recently more advanced models have been proposed in which the cement paste morphology is represented in several levels. Effective media theories are then utilized for obtaining effective diffusivities at each of these levels under the assumption of scale separation between two levels. Bary and Bejaoui [122] conceptualized the cement paste morphology as a three-coated sphere around a central core. Unhydrated clinkers form the core with layers of hydration products around it. The hydration products are divided into an inner and outer layer, the latter being further divided into an intermediate and an external shell. The inner layer is formed of HD C-S-H whereas the outer layer is formed of LD C-S-H and capillary pores. In both layers, minor hydration phases (portlandite (CH) and aluminate phases (AFm)) are present as spherical inclusions with a fraction proportional to the HD and LD C-S-H fractions in cement paste. CH and AFm are distributed equally in the intermediate and external shell, but these shells differ in capillary pores: non-percolated capillary pores in the intermediate shell and percolated capillary pores in the external shell. They assumed a percolation threshold for capillary pores as 8%. The effective diffusivity of this assembly is obtained based on the self-consistent approximation for multi-coated spheres proposed by Milton [144]. According to this theory, effective diffusivity ($D_{e,n}$) of a composite consisting of a n layer multi-coated sphere can be determined iteratively, wherein, at each iteration, the effective diffusivity of a single-coated sphere with a core consisting of an effective medium obtained in the previous iteration surrounded by the layer of the current iteration [144]

$$D_{e,n} = D_n + \left(1 - \frac{\phi_n}{\sum_{i=1}^{n} \phi_i}\right)\left[\frac{1}{D_{e,n-1} - D_n} + \frac{1}{3D_n}\frac{\phi_n}{\sum_{i=1}^{n}\phi_i}\right]^{-1} \quad (25)$$

where $D_{e,n}$ is the effective diffusivity determined for nth layer [$L^2\,T^{-1}$]; ϕ_i is the volume fraction of ith layer and $D_{e,n-1}$ is the effective diffusion coefficient of assembly of multicoated spheres consisting of $n-1$ layers [$L^2\,T^{-1}$]. The diffusivity for inner layer and the intermediate shell in Bary and Bejaoui [122] model are then determined by the Maxwell approximation and the diffusivity of external shell is determined using the self-consistent scheme to better represent the effect of percolation. The volume fractions of different phases are determined using Tennis and Jennings model [126]. The diffusivity of the LD and HD C-S-H were determined by fitting the HTO experimental data of Bejaoui et al. [145] as 3.4×10^{-12} m^2/s and 8.3×10^{-13} m^2/s, respectively. A similar conceptualization of cement paste morphology has been proposed by Stora et al. [123] but without the distinction between an intermediate and external shell in the outer layer. Diffusivities of both layers were determined using Maxwell's approximation and the effective diffusivity of LD and HD C-S-H was calculated using the mixed coated sphere assemblage model (MCSA) [146]. The MCSA scheme allows for better capturing of sudden variations in effective diffusivity caused by percolation effects compared to the self-consistent scheme. The MSCA model requires an additional fitting parameter known as the geometric parameter (f) which was determined as 0.805 and 0.546 for HD C-S-H and LD C-S-H, respectively. This model has been further extended to simulate the leaching of cement paste [147]. Dridi [124] also utilized the effective media theory for an assembly of multi-coated spheres to compute effective diffusivity of cement paste. He used a similar morphological conceptualization as Stora et al. [123] except that when the LD C-S-H volume fraction is smaller than the percolation threshold (e.g. for low w/c ratio), cement is represented as a single-coated sphere with LD C-S-H inclusions in the HD C-S-H layer. Similar to Stora et al. [123] the diffusivity of the inner and outer layers is computed using the generalized Maxwell approximation. To account for the percolation behaviour of capillary pores, the self-consistent scheme was used for the outer layer when capillary pores percolate. The percolation threshold for capillary pores was assumed to be 15%. The diffusivity of LD and HD C-S-H was obtained as 6.5×10^{-12} m^2/s and 1.25×10^{-12} m^2/s, respectively, by fitting with experimental results of Bejaoui and Bary [99]. These values are in a similar range as the one fitted by Bary and Béjaoui [122] for same experimental data.

Liu et al. [125] represented the morphology of cement paste in a rather different way. They considered cement paste morphology at three levels. At level I, they assumed the representation of two types of C-S-H, LD and HD C-S-H, both composed of non-diffusive spherical solid phase inclusions in the gel pore space. At level II, the porous C-S-H gel is composed of spherical inclusions of HD C-S-H and capillary pores smaller than 1 μm in the matrix of LD C-S-H. Finally, at level III, the cement paste itself is considered consisting of spherical inclusions of unhydrated cement, portlandite, aluminates and capillary pores in the matrix of the porous C-S-H gel. The diffusion coefficient of LD and HD C-S-H at level I is then determined using the differential effective media scheme. The diffusivity at level II and level III is determined using Maxwell's approximation and the self-consistent scheme, respectively. They determined the diffusivity of ions in gel pores to be 3×10^{-11} m^2/s by comparing with the steady-state diffusivity of chloride ions measured using electro-migration technique. The volume fractions of different phases were determined using the hydration model proposed by Bernard et al. [127]. The porosity of LD C-S-H and HD C-S-H in their model were kept constant for different w/c ratio with values as 0.37 and 0.24, respectively, which is based on the colloid model for C-S-H proposed by Jennings [25].

3.2. Effective diffusivity models for mortar and concrete

For mortar and concrete, the effect of ITZ and aggregates on diffusivity needs to be considered in addition to cement paste. Similar to cement paste, the models for mortar and concrete can be classified as empirical or analytical models derived from effective media theory. The models selected for discussions are summarized in Table 5. Empirical models similar to the ones described in Section 3.1 for cement paste have also been used for mortar and concrete. Some authors have fitted Archie's relationship to experimental data for mortars [91,101]. Tumidajski et al. [91] however concluded that Archie's relationship is less accurate compared to cement paste system. Nevertheless, Nokken and Hooton [101] obtained reasonable fits with Archie's relationship for a specific concrete mixture and concluded that there is no unique parameter set for Archie's relationship for all types of concrete mixtures. The porosity in most of these experiments has been determined using MIP. Halamickova et al. [148] tried to relate effective diffusivity of mortars with the critical pore radius, r_c (steepest slope of a cumulative porosity curve). The critical pore radius depends both on w/c ratio and

Table 5
Summary of effective diffusivity models for mortar and concrete.

Models/reference	Effective diffusivity of cement paste	Effective diffusivity of concrete	Fitting Parameters
Empirical models			
Archie's relationship [91]; Nokken and Hooton [101]	–	$D_e^{m/c} = A\phi^n$	A, n
Halamickova et al. [148]	–	$D_{con} = a_1 + a_2 r_c$	a_1, a_2
Effective media theories			
Constant diffusivity in ITZ			
Differential scheme [150] Schwartz, Garboczi and Bentz [150]	Input parameter	$\phi_{agg} = 1-(\frac{D_e^{m/c}}{D_e^p})^{g/e}(\frac{kD_e^{m/c}+e}{kD_e^p+e})^{(g/e-f/k)}$ $g = 2(D_e^{itz})^2(1-[\frac{r_{agg}}{r_{agg}+t_{itz}}]^3)$ $f = 2D_e^{itz}(2+[\frac{r_{agg}}{r_{agg}+t_{itz}}]^3)$ $e = 6(D_e^{itz})^2(-1+[\frac{r_{agg}+t_{itz}}{r_{agg}}]^3)$ $k = 3D_e^{itz}(-1+2[\frac{r_{agg}+t_{itz}}{r_{agg}}]^3)$	D_e^{itz}, r_{agg}, t_{itz}
Self-consistent scheme [150] Schwartz, Garboczi and Bentz [150]	Input parameter	$\frac{D_e^{m/c}}{D_e^p} = 1-\phi_{agg}\frac{1}{H}+\phi_{itz}(\frac{D_e^{itz}}{D_e^p}-1)\frac{2}{3H}$ $H = \frac{1}{9D_e^{itz}D_e^{m/c}}[2D_e^{itz}(D_e^{itz}+2D_e^{m/c})+\frac{2r_a{}^3}{(r_a+t_{itz})^3}D_e^{itz}(D_e^{m/c}-D_e^{itz})]$	D_e^{itz}, r_{agg}, t_{itz}
Maxwell's approximation (Care [151])	Input parameter	$D_e^{m/c} = D_e{}^p[a_1+(1-\phi_{agg})]\frac{2}{(2+\phi_{agg})}$	$a_1 = 0.11\phi_{itz}$, D_e^{itz}
Multi coated sphere assembly model (Care and Herve [152])	Input parameter	$D_e^{m/c} = D_e^p\frac{6D_e^p(1-\phi_{agg})(\phi_{agg}+\phi_{itz})+2\phi_{itz}(D_e^{itz}-D_e^p)(1+2\phi_{agg}+2\phi_{itz})}{3D_e^p(2+\phi_{agg})(\phi_{agg}+\phi_{itz})+2\phi_{itz}(1-\phi_{agg}-\phi_{itz})(D_e^{itz}-D_e^p)}$	D_e^{itz}
Composite spheres assemblage model (Oh and Jang [97])	Generalized self-consistent scheme – see Table 2 under Oh and Jang (2004)	$D_e^{m/c} = D_e^p[1+\frac{\phi_{agg}}{\frac{1}{2(D_e^{itz}/D_e^p)(t_{itz}/r_{agg})-1}+\frac{1-\phi_{agg}}{3}}]$	ϕ_{itz}, D_e^{itz}/D_e^p
Stora et al. [153]	see Table 2 under Stora et al. (2008)	$D_e^{m/c} = 2D_e^p(\frac{3}{2+\phi_{agg}-2\phi_{itz}\beta_{itz}^{agg}}-1)$ $D_e^{itz} = D_{LD-CSH}(\frac{1+2\sum_i\frac{\phi_i}{\phi_{LD-CSH}}\beta_{LD-CSH}^i}{1-\sum_i\frac{\phi_i}{\phi_{LD-CSH}}\beta_{LD-CSH}^i})$ i∈[CH, AF, CP] $\beta_i^j = \frac{D_i-D_j}{D_i+2D_j}$	t_{itz} (used for computing ϕ_{itz}), *hydration degree* (used for computing volume fractions of different phases such as CH, AF, CP in ITZ)
Single coated sphere model combined with an n-component anisotropic and percolating mixture model [154]	Input parameter	$D_e^{m/c} = \frac{D_e^pD_{ea}+2\phi_{paste}D_e^pD_{hm}+2\phi_{ea}D_{ea}D_{hm}}{\phi_{ea}D_e^p+\phi_{paste}D_{ea}+2D_{hm}}$ $D_{hm} = w_pD_e^p+w_{ea}D_{ea}$ $w_{ea} = \frac{(\phi_{ea}-\phi_{ea,c})^mH(\phi_{ea}-\phi_{ea,c})}{\phi_{paste}^m+(\phi_{ea}-\phi_{ea,c})^mH(\phi_{ea}-\phi_{ea,c})}$ $w_p = \frac{\phi_{paste}^m}{\phi_{paste}^m+(\phi_{ea}-\phi_{ea,c})^mH(\phi_{ea}-\phi_{ea,c})}$	$m = 1.75$; D_e^{itz}, $f_{ea,c}$
Varying diffusivity in ITZ			
Transfer matrix method [155]	Effective medium model for an anisotropic media and percolating mixture by Koelman and Kuijper [156] $D_e^p = \frac{2\phi_{tot}^{a_1}D_p}{\phi_{tot}^{a_2}(3-\phi_{tot})+a_3(1-\phi_{tot})^{a_1}}$	$D_e^{m/c} = -\frac{T_{21}r_c}{T_{11}}$ $[\boldsymbol{T}] = \prod_{i=1}^{N+1}t_{(N+2-i)}$ (2x2 matrix with T_{11}, T_{12}, T_{21} and T_{22} as components) $[t^i] = \begin{bmatrix} \frac{r_i^3+2r_{i+1}^3}{3r_ir_{i+1}^2} & \frac{r_i^3-r_{i+1}^3}{3D_{e,i}^pr_{i+1}^2} \\ \frac{2D_{e,i}^p(r_i^3-r_{i+1}^3)}{3r_ir_{i+1}^3} & \frac{2r_i^3+r_{i+1}^3}{3r_{i+1}^3} \end{bmatrix}$	Porosity gradient and t_{itz} (required to compute effective diffusivity of ITZ layers); a_1, a_2, a_3, D_p
MCSA [124]	See Table 2 under [124]	D_e^{itz} for each layer within ITZ region is computed based on the same cement paste model, see Table 2 under [124] $D_e^{m/c}$: same as Eq. (14)	ϕ gradient in ITZ and ϕ at the aggregate surface (used to compute volume fraction of LD C-S-H, HD C-S-H and CH-AF phases in ITZ, required in the effective diffusivity equation shown in Table 2 [124])

degree of hydration. This link was inspired from the Katz-Thompson relationship, which was originally proposed to relate conductivity of rocks with the critical pore radius [149]. For a w/c ratio equal to 0.5, a linear fit was found between diffusivity and critical pore radii. However, at a lower w/c ratio (w/c = 0.4) the linear fit was less accurate. All the empirical models do not account for the individual contributions of aggregates, ITZ and cement paste as these contributions are all lumped together in the fitting parameters.

Models utilizing effective media theory have also been proposed to predict diffusivity of concrete. These models conceptualize the concrete system with assembly of multicoated spheres with aggregates as core surrounded by layers of ITZ and cement paste. These models can be further distinguished into those that assume a constant diffusivity and those that assume a diffusivity gradient within ITZ; the latter because of a gradient in porosity generally observed in Scanning Electron Microscope (SEM) images of ITZ in concrete.

First the models with a spatially uniform diffusivity within the ITZ region are discussed. Starting from dilute limit composite theory (volume fraction of aggregates <5%), Schwartz et al. [150] proposed a differential as well as self-consistent effective media theory to compute effective diffusivity for larger volume fractions of sand. The performance of these models was compared against numerical random walk simulations carried out on four grain size (500, 1000, 1500 and 3000 μm) random sphere packing structure, with 54% volume fraction of sand and a constant ITZ thickness of 20 μm. Good comparisons were achieved for both theories for volume fractions of up to 60%, provided the ratio of ITZ diffusivity (D_e^{itz}) to cement paste diffusivity (D_e^p) was below 20. However, in a later work, Garboczi and Bentz [157] adopted the transfer matrix method proposed by Herve and Zaoui [158] to determine effective diffusivity of mortar system. In this approach, ITZ is subdivided into '*N*' number of layers, each with a different property. For such a system, they provided an analytical solution only for the dilute limit, which can then be extended to arbitrary volume fractions via differential or self-consistent schemes described by Schwartz et al. [150].

Care [151] proposed a model that takes into account the effect of ITZ and tortuosity introduced by aggregates, which is an improved form of effective diffusivity relationship proposed by Christensen [159] that

only accounted for aggregates. The main assumption is that the tortuosity parameter only depends on the volume fraction of aggregates and not on aggregates size distribution. They used Maxwell's approximation to consider the effect of aggregates only (aggregates-cement paste system). However, to accommodate the effect of ITZ, they empirically added a term to Maxwell's approximation for aggregate-cement paste system. Thus their method could be classed as semi-analytical with two parameters to be fitted; D_e^{itz} and a parameter m (see Table 5 for the mathematical form). They were able to demonstrate the capability of the model against their own experiments of chloride diffusivity for mortars with a maximum error of 16%. All mortars had a w/c ratio equal to 0.45, but two different volume fractions of aggregates were used (0.25 and 0.5). In a further work, Care and Herve [152] adopted (n + 1) phase model proposed earlier by Herve [160] to derive an effective diffusivity model for concrete, which is effectively the multicoated sphere model (see Section 3.1) proposed by Milton [161]. Care and Herve [152] used the same experiments as in Care [151] to demonstrate the validity of their model. Clearly, the main conclusion from their work is that significant differences (i.e. up to 76% error for the experiments considered) with respect to measured data will result if ITZ is not considered. However, note that because of the fact that D_e^{itz} cannot be directly measured, they determined it by comparing with the predictions of the model with experimental data. This essentially means that there is uncertainty even in the D_e^{itz} parameter.

Oh and Jang [97] adopted a composite spheres assemblage model proposed by Hashin [162] to include the effect of ITZ and aggregates in their effective diffusivity model. This model requires the volume fraction of aggregates, the ratio of ITZ thickness (t_{itz}) to average radius of aggregate particles (r_a) and D_e^{itz}/D_e^p ratio as input parameters. D_e^{itz} is computed from the knowledge of the porosity of ITZ (ϕ_{itz}) using the general effective medium theory for cement paste described in Section 3.1. The accuracy of their model predictions depends on the assumptions made concerning D_e^{itz}/D_e^p, ITZ thickness and D_e^p, which itself depends on the percolation exponent and solid phase diffusivity of C-S-H (Section 3.1). For validation with experimental data, they assumed the porosity of ITZ to be 1.5 times that of capillary porosity of cement paste based on experimental data of Bourdette et al. [163]. D_e^{itz}/D_e^p ($\approx$7) and ITZ thickness ($\approx$20 μm) were fitted to the experimental data. They were able to demonstrate reasonably good agreement with experimental diffusivity for both mortar and concrete with various cement types, viz., ordinary Portland cement, sulphate resistant Portland cement, fly ash and blast furnace slag with varying water to binder ratios (0.35 to 0.55).

Stora et al. [153] proposed a multi-scale modelling framework in which a series of micromechanical models were implemented to estimate the effective diffusivity of mortars. In particular, they use interaction direct derivative (IDD) estimates (Zheng and Du [164], which is the same as Maxwell's approximation for spherical inclusions) to compute the D_e^{itz} and a multi-coated sphere model proposed by Milton [161] to estimate the diffusivity of hardened cement paste (see Section 3.1) as well as mortar. The ITZ is conceptualized as consisting of CH, AF and capillary pore inclusions within LD C-S-H matrix. While all the models presented above consider porosity and hence diffusivity as an input parameter, Stora et al. [153] proposed a different approach to compute the average porosity of ITZ. Firstly, they compute the compositions of the mortar and of its bulk cement matrix that is assumed to be identical to the plain hardened cement paste via Tennis and Jennings [126] hydration model. The hydration degree is then adjusted to retrieve the measured water porosities for the mortar and plain hardened cement paste. The volume fractions of phases within ITZ are then deduced as the difference between the volume fraction in the mortar and the volume fractions in the cement matrix. In this way, they come to an average porosity of 70% in the ITZ for a particular experiment, which is used in the IDD estimate to compute D_e^{itz}. Based on Heukamp [165], Stora et al. [153] assumed the ITZ thickness to be 20 μm for their simulations. Comparison of the model results for effective diffusivity against the experimental data of Bourdette [166] and le Bellego [167] showed an error of 6%.

To derive average porosity in the ITZ, another interesting way was proposed much earlier by Bentz and Garboczi [168] who used a micro-scale cement hydration model. This essentially involves randomly generating cement particles within a small computational volume in which the ratio of volume of bulk cement paste and ITZ are pre-defined and hydrated to a desired degree. Their model computes porosity distribution both in the ITZ and bulk cement paste. Average porosity is then calculated for each region and is used in a diffusivity-porosity relationship to obtain effective diffusivity of ITZ and bulk cement paste.

Zheng and Zhou [154] combined the single-coated sphere diffusivity model [169] with an effective medium model for percolating mixture proposed by Koelman and Kuijper [156]. Using the single-coated sphere model, they essentially determined the effective diffusivity of an aggregate and ITZ system (or a so-called equivalent aggregate system). This information was then introduced into another two-phase system comprising equivalent aggregates and cement paste. To solve the resultant system, they used the Koelman and Kuijper's [156] effective medium model for percolating mixture, which specifically takes into account percolation of multiple phases and is applicable over arbitrarily wide range of volume fractions of the components. The latter model possesses advantages of both the differential and self-consistent schemes, in particular, over the entire diffusivity contrast range between the phases. As stated by Koelman and Kuijper [156], their approach is better than differential effective medium theories that describe inclusions as disjoint phases in a continuous matrix, i.e. percolation is allowed in only one phase. It also out performs self-consistent schemes because the latter results in unrealistic percolation threshold for two phases with highly contrasting properties. Key parameters that are needed in Zheng nd Zhou's [154] model are the D_e^{itz} and a percolation exponent m. They determined the D_e^{itz} through inverse analysis of an experiment, whereas, an average value of percolation exponent was obtained (m = 1.75) from fitting Archie's law to glass bead experiments [170]. Comparisons with their own experiments on concrete over a range of volume fractions proved successful with only 6% error.

In the following, models that consider varying diffusivity within the ITZ region are presented. Zheng et al. [155] use the multi-coated sphere assemblage concept and adopted the transfer matrix method proposed by Herve and Zaoui [158] to estimate the effective diffusivity of the composite structure consisting of aggregates, ITZ layers and cement paste layer. In this aspect, their work is similar to that of Garboczi and Bentz [157], who demonstrated the use of transfer matrix method to derive the effective diffusivity of concrete under a dilute limit assumption. Zheng et al. [155] considered variation in capillary porosity within ITZ based on a power law with respect to distance from the aggregate surface obtained by fitting experimental data of Crumbie [121]. This power law is derived in such a way that ITZ thickness is left as a free parameter, which allows for sensitivity analysis of this parameter. Through sensitivity analysis they showed that a minimum of six layers suffices to reach convergence of the effective diffusivity of the entire ITZ. The diffusivity models for ITZ as well as for cement paste are based on Zheng and Zhou [171], who used the work of Koelman and de Kuijper [156] (see Table 5). Using the actual aggregate size distribution and cement composition from Delagrave et al. [172] and Yang and Su [173] for mortars, they were able to demonstrate good correspondence with measured diffusivity for various volume fractions of aggregates for samples with w/c ratio of 0.25, 0.4 and 0.45, with the exception of the 0.38 sample. The important input parameters necessary for all these simulations are ITZ thickness, which was assumed on the basis of w/c ratio, and the D_e^p, which was in fact fitted based on the above experimental data. The fitting parameters used in the D_e^p equation are: $a_1 = 2.75$, $a_2 = 1.75$ and $a_3 = 14.4$ (Table 5). Even though free water diffusion for chloride ions is known, the pore diffusion coefficient D_p is not known because of pore geometry effects and thus D_p was also calibrated from experiments. Nevertheless, their main conclusion was that the influence of

ITZ on the overall diffusivity was not too significant, even though on average it is more porous and its diffusivity is higher than that of the cement paste.

Dridi [124] adopted the $(n+1)$ phase model for concrete proposed by Care and Herve [152], which is effectively the multi coated sphere model by Milton [161]. However, Dridi [124] further considered the variation in capillary porosity within ITZ based on the power relationship used by Zheng et al. [155]. As in Zheng et al. [155], they subdivided the ITZ layer into a number of layers (number not specified) and determined diffusivity of each ITZ layer via a self-consistent or Maxwell scheme depending upon whether pores reach percolation or not. The same analytical schemes were also used for the cement paste layer. The diffusivities available for each layer were then used to compute the effective diffusivity of concrete. Note that in their ITZ model, not only the power relationship for capillary porosity is fitted based on an experimental data but also the capillary porosity at the aggregate surface is assumed to be 2.5 times that of cement paste. They demonstrated a very good agreement with the experimental HTO diffusivity determined by Delagrave et al. [85] and Tognazzi [174] for mortars and Lamotte and Le Cocguen [175] for concrete. Due to a lack of experimental data, they numerically explored the effect of ITZ on the effective diffusivity of concrete and suggested its dominant role.

To summarize, one can conclude that it is not possible to have a unique empirical model that can predict effective diffusivity of any mortar/concrete system. Calibration will always be necessary with specific set of experiments because mortar/concrete is treated as a single homogeneous system. On the other hand, the use of analytical models based on effective media theory is promising. However, even with this approach there are always parameters that need to be calibrated with experiments, specifically, diffusivity, porosity and thickness of ITZ and for some models the degree of hydration (Stora et al. [153]) and exponents (Zheng and Zhou [154]). In fact, the accuracy of effective diffusivity of mortar/concrete is highly dependent on the cement paste diffusivity. Thus uncertainties associated with cement paste diffusivity models also contribute to the overall uncertainty of the diffusivity models of mortar/concrete. For some models, ITZ diffusivity is calculated based on capillary porosity relationship for ITZ. The porosity relationship for ITZ depends upon various factors such as cement type and composition, w/c ratio and volume fraction of aggregates. Therefore, specific caution has to be exercised in the choice of the ITZ porosity relationship for a given material. Another important issue not to be overlooked is when dividing ITZ into a number of sub-layers to determine the effective diffusivity of ITZ. In doing so, the thickness of each ITZ sub-layer will be reduced to just a few microns, in which case there may not be a representative volume element to determine effective diffusivity of each sub-layer. Finally, with so many models that aim to capture the effect of ITZ and aggregates, it is clear that there is no unique conclusion on the role of ITZ in the overall diffusivity of mortar/concrete systems. For example, Care and Herve [152], state that there could be up to 76% error in model prediction vis-à-vis experimental results if ITZ is not considered. Dridi through numerical analysis showed the effect of increased ITZ thickness on the increased effective diffusivity of mortar. Whereas, Zheng et al. [155] concluded that ITZ effect on the overall diffusivity was not too significant, even though on average it is more porous and its diffusivity is higher than that of the cement paste. They further conclude that this indicates that diffusivity is governed by the volume fraction and pore structure of cement paste and not just that of porous ITZ.

3.3. Comparison of effective diffusivity relationships for cement paste

As discussed in Section 2.3.2, the experimental data for diffusivity of mortar and concrete depends predominantly on the diffusivity of the cement paste and aggregate fraction. It is therefore of primary importance to test and compare the predictive capabilities of different effective diffusivity models for cement paste on the larger dataset compiled in Section 2.3.1 using the parameters proposed by the authors and which are summarized in Table 6. For the empirical relationships discussed in Section 3.1, it is more relevant to compare the quality of the relationship rather than its predictive capabilities. Hence, for these relationships, unknown parameters are calibrated with the experimental data collected in Section 2.3.1. For models that require volume fractions of different phases the comparisons were carried out only for a selected set of experimental data given in Table 7, excluding the experimental data that were used to calibrate the relationships by the respective authors. The volume fractions of different phases were computed using the Tennis and Jennings hydration model [126] and reported in Table 7. For the models of Liu et al. [125] and Stora et al. [123], we specifically consider porosities of LD C-S-H and HD C-S-H as 0.37 and 0.24, respectively, which are based on the colloid model of C-S-H proposed by Jennings [25]. Consequently, the remaining parameters of Stora et al. [123] model had to be recalibrated using the experimental data of Bejaoui and Bary [99] (which was used in Stora et al. [123]) as the above porosity values are different from those used in their paper.

Figs. 8, 9 and 10 compare the relative diffusivity obtained using different types of models and experimental data. Fig. 8 groups the empirical models. Fig. 9 groups two models accounting for morphological nature of cement paste in a simplified way and that which express the relationship solely in terms of capillary porosity, i.e. the NIST model [14] and Generalized effective media theory [97]. Models that take into account detailed morphological aspects of cement paste are grouped in Fig. 10. Table 8 summarizes the percentage of data for which the estimated relative diffusivity is within factor 2-bounds of the measured value. As discussed in Section 2.3, electro-migration data has the smallest scatter with all data falling within a factor of two of the fitted relationship. Hence, this factor serves as a good indicator to quantitatively compare different models.

Fig. 8 reveals that all the empirical relationships viz., Archie's relationship and exponential relationship between capillary porosity and relative diffusivity, and exponential relationship between w/c and relative diffusivity (at maximum hydration degree) have almost the same

Table 6
Parameter values used for different relative diffusivity models of cement paste.

Reference/model	Parameters used
Archie's relationship[a]	A: 0.0462, 0.1158, 0.5385 for electro-migration, through-diffusion and electrical resistivity respectively n: 1.3916, 2.0609, 2.3366 for electro-migration, through-diffusion and electrical resistivity respectively
Exponential form [21,119][a]	A: 0.0006, 0.0003 and 0.0021 for electro-migration, through-diffusion and electrical resistivity respectively n: 9.7627, 11.507 and 8.2079 for electro-migration, through-diffusion and electrical resistivity respectively
Exponential form with respect to water cement ratio [120][a]	A: 0.002,0.00007 and 0.0002 for electro-migration, through-diffusion and electrical resistivity respectively n: 3.4779, 8.2253 and 6.3193 for electro-migration, through-diffusion and electrical resistivity respectively
NIST model [14]	A_1: 1.7, A_2: 0.03, A_3: 0.0004 and ϕ_c: 0.2
Generalized self-consistent scheme [97]	D_s: $2\times10^{-5}D_0$, n: 2.7 and ϕ_c: 0.17
Bejaoui and Bary [99]	D_{LD-CSH}: $4.0179\times10^{-3}D_0$, D_{HD-CSH}: $4.4643\times10^{-4}D_0$
Bary and Bejaoui [122]	D_{LD-CSH}: $1.7\times10^{-3}D_0$, D_{HD-CSH}: $4.15\times10^{-4}D_0$
Stora et al. [123][b]	f_{gp}^{LD-CSH}: 0.675, f_{gp}^{HD-CSH}: 0.761
Dridi [124]	D_{LD-CSH}: $2.9018\times10^{-3}D_0$, D_{HD-CSH}: $5.35714\times10^{-4}D_0$
Liu et al. [125]	D_{gp}: $1.8634\times10^{-2}D_0$

[a] Parameters were calibrated to the compiled experimental data presented in Section 2.3.1.
[b] Parameters were re-calibrated to the experimental data of Bejaoui and Bary [99].

Table 7
Volume fractions of different phases of cement paste computed using the Tennis and Jennings hydration model for selected experimental datasets.

References	w/c	Degree of hydration	Clinkers	Portlandite	Aluminates	Capillary porosity	HD C-S-H	LD C-S-H
Migration								
Sun et al. [96]	0.23	57.7[a]	22.3	10.83	17.19	4.5	35.75	8.36
	0.35	78.0[a]	9.38	12.41	19.37	10.79	31.86	17.45
	0.53	28.05[a]	2.66	10.92	17.42	20.01	10.0	40.84
Oh and Jang [97]	0.35	78.1[a]	10.11	7.12	28.04	7.3	30.64	16.79
	0.45	87.8[a]	4.91	6.77	25.01	12.28	20.67	30.37
	0.55	93.01[a]	2.46	6.33	22.09	17.2	7.55	44.36
Through-diffusion								
Delagrave et al. [85]	0.45	87.8[a]	4.93	15.79	14.67	13.6696	20.63	30.31
	0.25	61.8[a]	21.21	14.52	14.84	4.4291	35.9451	9.05
Yamaguchi et al. [88]	0.45	87.8[a]	4.87	10.60	23.17	13.2694	19.47	28.61
	0.6	94.6[a]	1.79	9.21	19.63	20.7149	9.48	47.69
	0.75	97.11[a]	0.83	8.05	16.85	27.3181	0	43.39
Ngala et al. [95]	0.4	83.64[a]	6.99	11.33	21.93	10.44	26.09	23.02
	0.5	90.9[a]	3.44	10.61	20.25	15.7	13.74	36.26
	0.6	94.6[a]	1.79	9.69	18.03	20.5	0.97	49.02
	0.7	96.6[a]	1.04	8.84	16.24	24.97	0	48.91
Phung [48]	0.425	85.9[a]	5.83	13.18	19.48	12.71	22.9	25.91
Electrical resistivity								
Ma et al. [92]	0.3	52.2	24.3	9.05	15	16.95	22.6	12.16
	0.3	61	19.78	10.73	17.65	11.90	27.63	12.32
	0.3	65	17.71	11.50	18.83	9.64	30.08	12.23
	0.4	51	21.41	7.58	12.56	28.33	14.60	15.51
	0.4	63.1	16.06	9.57	15.70	21.9	18.45	18.31
	0.4	70	13.01	10.72	17.41	18.29	20.76	19.81
	0.4	72	12.13	11.05	17.89	17.25	21.44	20.23
	0.5	56	16.83	7.36	12.17	33.88	9.74	20.02
	0.5	67	12.57	8.95	14.62	28.38	11.02	24.46
	0.5	74	9.86	9.98	16.10	24.90	11.75	27.41
	0.5	79	7.93	10.71	17.12	22.43	12.23	29.58

[a] Degree of hydration is computed using the maximum degree of hydration equation proposed in Ref. [99].

level of accuracy once they are calibrated to the data compiled in Section 2.3. This is confirmed by percentage of estimates lying within factor 2-bounds (Table 8), which is above 70% on average after calibration. Each relationship has to be calibrated separately for through diffusion, electro-migration and electric-resistivity to achieve good fit.

Simplified models viz., Oh and Jang model [97] based on generalized effective media theory and NIST model derived from computer simulations have been compared in Fig. 9. Oh and Jang model performs better than NIST model for electro-migration (see Fig. 9 and Table 8) as parameters for Oh and Jang model has been calibrated with electro-migration data. Oh and Jang model also performs slightly better than NIST model for other type of experiments. In spite of different conceptual approaches both models have similar predictability and >49% of the estimated values of both models (neglecting the performance of Oh and Jang's model for electro-migration) lie within factor 2-bounds. The parameters in both models have physical meaning, however, they cannot be easily measured and hence to improve predictability the

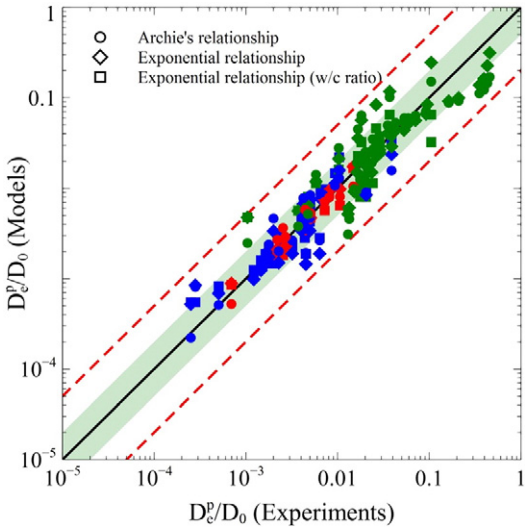

Fig. 8. Comparison of relative diffusivity obtained from empirical relationships and experimental data. Blue, red and green markers represent through-diffusion, electro migration, and electro resistivity, respectively. Shaded green region shows factor of 2 bound and dashed line shows factor of 5 bounds.

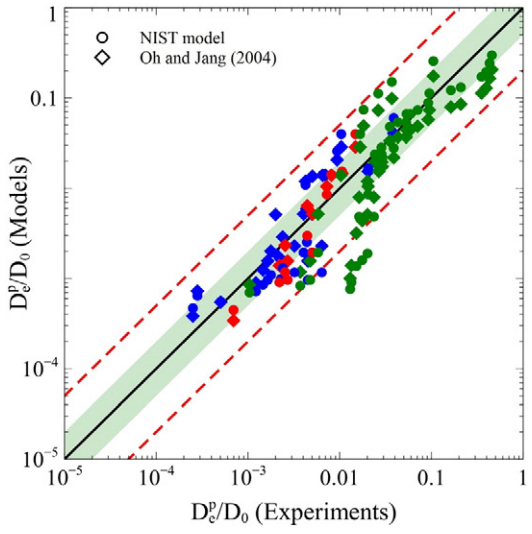

Fig. 9. Comparison of relative diffusivity obtained from models that depend only on capillary porosity and experimental data. Blue, red and green markers represent through-diffusion, electro migration, and electrical resistivity, respectively. Shaded green region shows factor of 2 bounds and dashed line shows factor of 5 bounds.

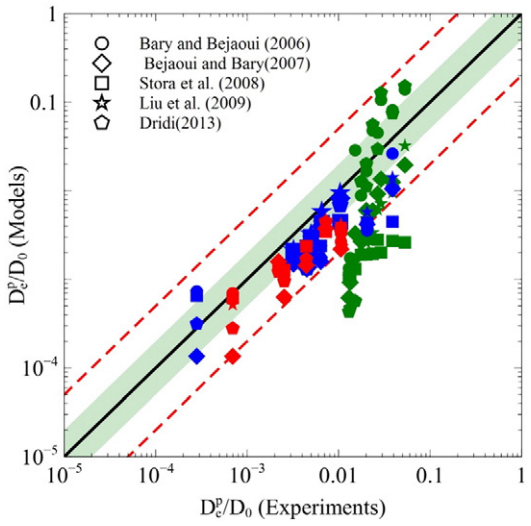

Fig. 10. Comparison of relative diffusivity obtained from models that take into account morphology of cement paste in detail and experimental data. Blue, red and green markers represent through-diffusion, electro migration and electrical resistivity, respectively. Shaded green region shows factor of 2 bounds and dashed line shows factor of 5 bounds.

parameters of these models need to be recalibrated on larger dataset. Moreover, both models under predict the relative diffusivity for the electrical resistivity data at low relative diffusivity (i.e. lower capillary porosity or w/c ratio) with some data points lying beyond factor 5-bounds. As mentioned in Section 2.3.1, the relative diffusivity obtained from electrical resistivity measurements is higher than those obtained from the other methods at lower capillary porosity. Differences in results between the two models originate due to the fact that these models have been calibrated either with data from through-diffusion or electro-migration. Therefore, for electric resistivity experiments the parameters for these models need to be re-calibrated.

Amongst the models taking into account detailed morphological aspects, the Bejaoui and Bary [99] model that is based on set of series/parallel configurations shows least agreement (Table 8). For electro-migration, the multi-coated sphere based models of Bary and Bejaoui [122] and Stora et al. [123] performs slightly better than multi-coated sphere based model of Dridi [124] with 50% or more predictions (of 6 data points) lying within a factor 2-bounds. This difference is specifically at low diffusivity (low capillary porosity). Recall that Dridi's model assumes cement paste morphology as single coated sphere whereas the other two assume cement paste morphology as doubly coated sphere at low capillary porosity or w/c ratio. For through diffusion results, these three models perform equally (40% of 10 data points within factor 2-bounds) as the respective authors have calibrated them on the through diffusion data of Bejaoui and Bary [99]. Performance of Liu et al. [125] model, which is based on a rather different approach, wherein cement paste morphology is considered in three levels, is comparable to the multi-coated sphere based models of Bary and Bejaoui [122] and Stora et al. [123]. For electrical resistivity data, only the models of Bary and Bejaoui [122] and Dridi [124] show reasonable predictability with 45.5% of the predictions (of 11 data points) lying within factor 2-bounds of the experimental data. However, all models are less satisfactory for low relative diffusivities (see Fig. 10) with a large percentage of the predictions lying beyond a factor 5-bounds for the same reason explained above for the simplified models. All of these models conceptualize the cement paste morphology in detail and calibration parameters in these models are linked with C-S-H phase diffusivity. Hence, it can be speculated that differences between electrical resistivity measurements and through-diffusion or electro-migration are associated with the diffusivity of C-S-H phase. This is because at low capillary porosities or w/c ratio (i.e. low relative diffusivities), where these models fail to predict relative diffusivity accurately, C-S-H phase is the dominant transport phase.

In general one can conclude that advanced models have a better conceptualization of cement paste morphology. However, the parameters needed for these models are hard to determine directly by experiments and these models would need recalibration on a larger dataset. The calibration should be carried out differently for each technique as relative diffusivity values reported for different techniques can vary considerably as explained in Section 2.3. In this aspect empirical relationships are rather simple. We have recalibrated the empirical relationships (Table 8), which can be readily used for practical purposes keeping in mind that the uncertainty might be within factor 2-bounds. However, the value of the advanced models cannot be underestimated as they enable better understanding of the influence of the heterogeneities of cement paste on relative diffusivity.

4. Conclusions

This paper reviews different experimental techniques and modelling approaches for ordinary Portland cement based material under saturated conditions. A database of existing measured relative diffusivities obtained for cement paste, mortar and concrete serves as a basis to critically assess different measurement techniques and model predictions. For electrical resistivity and through-diffusion experiments, all the collected data for cement paste lie within a factor 5-bounds and factor of 4-bounds, respectively. For electro-migration experiments, the range is smaller with all data for cement paste falling within factor 2-bounds. This scatter between the values can arise from several reasons such as differences in cement composition, curing, maturity, experimental protocols and use of different tracers for through-diffusion experiments. It has been also observed that the relative diffusivities for cement paste, mortar and concrete obtained at low to moderate w/c ratio or capillary porosities obtained by electrical resistivity

Table 8
Percentage of data lying between factor 2-bounds for different relationship of relative diffusivity of cement paste - the number of experimental data considered in each case is represented in brackets.

Reference/model	Electro-migration	Through-diffusion	Electrical resistivity	Average
Archie's relationship	100[a](10)	72[a](25)	65[a](40)	72
Exponential form [21,119]	100[a](10)	76[a](25)	65[a](40)	73.3
Exponential form with respect to water cement ratio [120]	100[a](10)	76[a](25)	62.5[a](16)	76.5
NIST model [14]	50(10)	44(25)	52.5(40)	49.3
Oh and Jang model [97]	90[b](10)	56(25)	55(40)	60
Bejaoui and Bary [99]	33.3(6)	20(10)	0(11)	14.8
Bary and Bejaoui [122]	50(6)	40(10)	45.5(11)	44.5
Stora et al. [123]	67.7(6)	40(10)	0(11)	29.9
Dridi [124]	33.3 (6)	40 (10)	45.5(11)	40.75
Liu et al. [125]	50(6)	50(10)	9.1(11)	33.3

[a] These models have been calibrated on the experimental data presented in this paper and hence it shows good predictability compared to other models.
[b] Good predictability is due to the fact that this model has been fitted with electro migration test.

measurements are always larger (up to one order) than those obtained with the other methods. Electro-migration and through-diffusion techniques give similar diffusivity values for cement paste, however very few data points exists for cement paste for w/c ratio in the range of 0.25 to 0.3. For mortar/concrete, data points collected in the w/c ratio range from 0.25 to 0.3 reveals that relative diffusivity measured by electro-migration might be lower than by through-diffusion. The increase in relative diffusivity with w/c ratio and capillary porosity is obvious for cement paste. For mortar and concrete, increase in diffusivity with w/c ratio and decrease of diffusivity with an increase in the amount of aggregates for a given w/c ratio is observed, the latter being the consequence of an increased tortuosity. The mortar and concrete diffusivities, when normalized with cement paste diffusivity and plotted with respect to fraction of cement paste in the mortar/concrete, fall on a straight line irrespective of the study or the measurement method. All the data falls within a factor 1.5-bounds. This reveals that the relative diffusivity of mortar/concrete can be directly determined from the diffusivity of cement paste diffusivity and that the ITZ might have a limited to no influence on diffusion.

A large number of models have been proposed to predict effective diffusivity of hardened cement paste, mortar and concrete. None of these models are devoid of calibration of parameters. For cement paste, even the most advanced models require parameter associated with diffusivity in the gel pores of C-S-H. For mortar and concrete models, whether or not they are empirical, there are always parameters that need to be calibrated with relevant experiments, specifically, diffusivity, porosity and thickness of ITZ and for some models the degree of hydration and exponents, including parameters relevant to cement paste diffusivity models. Based on the discussed mortar/concrete models, it appears that there is no unique conclusion on the role of ITZ in the overall diffusivity of mortar/concrete systems. We believe that one could expect a dominant influence of ITZ only if there is a large contrast in the D_e^{itz}/D_e^p ratio. As the experimental data for mortar and concrete compiled in this study shows direct dependence on cement paste data and no influence of ITZ, comparison of only different cement paste models have been made in this study. All empirical models once calibrated to the data compiled in this study show similar predictive behaviour. Models accounting for cement paste morphology in simplified way and advanced models show a similar predictability. For accessing the predictability of these models same parameter as those proposed by the respective authors have been used. On average for most of the models 40% or more of the predicted data lies between factor 2-bounds. However, all these models are not able to well predict the electrical resistivity data, with predictions deviating by more than a factor of 5 for experimental data with a low relative diffusivity (capillary porosity). This is due to the fact that all these models have not been calibrated using electrical resistivity data. In order to utilize these models for practical purposes recalibration with larger dataset such as the one compiled in this study might be needed. Note that in this study we have only recalibrated empirical relationships and these relationships can be utilized for practical purposes keeping in mind that the uncertainty might be within factor 2-bounds.

Acknowledgements

The financial support by Belgian Nuclear Research Centre (SCK•CEN) is gratefully acknowledged. We would like to thank two anonymous reviewers for their constructive remarks which helped to substantially improve the quality of the paper.

References

[1] G.K. Glass, N.R. Buenfeld, Chloride-induced corrosion of steel in concrete, Prog. Struct. Eng. Mater. 2 (2000) 448–458.
[2] A. Neville, The confused world of sulfate attack on concrete, Cem. Concr. Res. 34 (2004) 1275–1296.
[3] C.F. Ferraris, P.E. Stutzman, K.A. Snyder, Sulfate resistance of concrete: a new approach, R&D Serial, 2006.
[4] Q.T. Phung, N. Maes, D. Jacques, E. Bruneel, I. Van Driessche, G. Ye, G. De Schutter, Effect of limestone fillers on microstructure and permeability due to carbonation of cement pastes under controlled CO2 pressure conditions, Constr. Build. Mater. 82 (2015) 376–390.
[5] Q.T. Phung, N. Maes, D. Jacques, G.D. Schutter, G. Ye, in: C. Hellmich, B. Pichler, J. Kollegger (Eds.),Evolution of Microstructure and Transport Properties of Cement Pastes Due to Carbonation under a CO2 Pressure Gradient - A Modeling Approach, CONCREEP 10, American Society of Civil Engineers, 2015, pp. 1032–1041.
[6] Q.T. Phung, N. Maes, D. Jacques, G. De Schutter, G. Ye, J. Perko, Modelling the carbonation of cement pastes under a CO2 pressure gradient considering both diffusive and convective transport, Constr. Build. Mater. 114 (2016) 333–351.
[7] Q.T. Phung, N. Maes, D. Jacques, G.D. Schutter, G. Ye, Decalcification of cement paste in NH_4NO_3 solution: microstructural alterations and its influence on the transport properties, in: J. Bastien, N. Rouleau, M. Fiset, M. Thomassin (Eds.),10th Fib International PhD Symposium in Civil Engineering, Québec, Canada 2014, pp. 179–187.
[8] Q.T. Phung, N. Maes, D. Jacques, G.D. Schutter, G. Ye, Microstructural and permeability changes due to accelerated Ca leaching in ammonium nitrate solution, in: M. Grantham, P.A.M. Basheer, B. Magee, M. Soutsos (Eds.), Concrete Solutions - 5th International Conference on Concrete Repair, CRC Press 2014, pp. 431–438.
[9] Q.T. Phung, N. Maes, D. Jacques, G. De Schutter, G. Ye, Investigation of the changes in microstructure and transport properties of leached cement pastes accounting for mix composition, Cem. Concr. Res. (2015).
[10] Q.T. Phung, N. Maes, D. Jacques, J. Perko, G. De Schutter, G. Ye, Modelling the evolution of microstructure and transport properties of cement pastes under conditions of accelerated leaching, Constr. Build. Mater. 115 (2016) 179–192.
[11] D. Jacques, N. Maes, J. Perko, S.C. Seetharam, Q.T. Phung, R. Patel, A. Soto, S. Liu, L. Wang, G.D. Schutter, G. Ye, K.v. Breugel, Concrete in engineered barriers for radioactive waste disposal facilities - phenomenological study and assessment of long term performance, 15th International Conference on Environmental Remediation and Radioactive Waste Management - ICEM2013, Brussels, Belgium 2013, pp. 1–10.
[12] G.V.D. Wegen, R.B. Polder, K.V. Breugel, Guideline for service life design of structural concrete: a performance based approach with regard to chloride induced corrosion, Heron, 57, 2012, pp. 153–168.
[13] C.D. Shackelford, D.E. Daniel, Diffusion in saturated soil 1. BACKGROUND, J. Geotech. Eng. ASCE 117 (1991) 467–484.
[14] E.J. Garboczi, D.P. Bentz, Computer simulation of the diffusivity of cement-based materials, J. Mater. Sci. 27 (1992) 2083–2092.
[15] P. Grathwohl, Diffusion in Natural Porous Media: Contaminant Transport, Sorption/Desorption and Dissolution Kinetics, Springer Science & Business Media, 2012.
[16] M. Aguayo, P. Yang, K. Vance, G. Sant, N. Neithalath, Electrically driven chloride ion transport in blended binder concretes: insights from experiments and numerical simulations, Cem. Concr. Res. 66 (2014) 1–10.
[17] J. Lizarazo-Marriaga, P. Claisse, Determination of the concrete chloride diffusion coefficient based on an electrochemical test and an optimization model, Mater. Chem. Phys. 117 (2009) 536–543.
[18] J. Arnold, D.S. Kosson, A. Garrabrants, J.C.L. Meeussen, H.A. van der Sloot, Solution of the nonlinear Poisson–Boltzmann equation: application to ionic diffusion in cementitious materials, Cem. Concr. Res. 44 (2013) 8–17.
[19] Y. Elakneswaran, A. Iwasa, T. Nawa, T. Sato, K. Kurumisawa, Ion-cement hydrate interactions govern multi-ionic transport model for cementitious materials, Cem. Concr. Res. 40 (2010) 1756–1765.
[20] Y. Ichikawa, K. Kawamura, N. Fujii, T. Nattavut, Molecular dynamics and multiscale homogenization analysis of seepage/diffusion problem in bentonite clay, Int. J. Numer. Methods Eng. 54 (2002) 1717–1749.
[21] A. Atkinson, A.K. Nickerson, The diffusion of ions through water-saturated cement, J. Mater. Sci. 19 (1984) 3068–3078.
[22] S. Goto, D.M. Roy, Diffusion of ions through hardened cement pastes, Cem. Concr. Res. 11 (1981) 751–757.
[23] K. Nakarai, T. Ishida, K. Maekawa, Modeling of calcium leaching from cement hydrates coupled with micro-pore formation, J. Adv. Concr. Technol. 4 (2006) 395–407.
[24] H.M. Jennings, Refinements to colloid model of C-S-H in cement: CM-II, Cem. Concr. Res. 38 (2008) 275–289.
[25] H.M. Jennings, A model for the microstructure of calcium silicate hydrate in cement paste, Cem. Concr. Res. 30 (2000) 101–116.
[26] K.L. Scrivener, A.K. Crumbie, P. Laugesen, The interfacial transition zone (ITZ) between cement paste and aggregate in concrete, Interface Sci. 12 (2004) 411–421.
[27] Y. Gao, G. De Schutter, G. Ye, Micro- and meso-scale pore structure in mortar in relation to aggregate content, Cem. Concr. Res. 52 (2013) 149–160.
[28] L. Liu, W. Sun, G. Ye, H. Chen, Z. Qian, Estimation of the ionic diffusivity of virtual cement paste by random walk algorithm, Constr. Build. Mater. 28 (2012) 405–413.
[29] L. Liu, H. Chen, W. Sun, G. Ye, Microstructure-based modeling of the diffusivity of cement paste with micro-cracks, Constr. Build. Mater. 38 (2013) 1107–1116.
[30] M.Z. Zhang, G.A. Ye, K. van Breugel, Microstructure-based modeling of water diffusivity in cement paste, Constr. Build. Mater. 25 (2011) 2046–2052.
[31] S. Kamali-Bernard, F. Bernard, W. Prince, Computer modelling of tritiated water diffusion test for cement based materials, Comput. Mater. Sci. 45 (2009) 528–535.
[32] M. Zhang, G. Ye, K. van Breugel, Modeling of ionic diffusivity in non-saturated cement-based materials using lattice Boltzmann method, Cem. Concr. Res. 42 (2012) 1524–1533.
[33] N. Ukrainczyk, E.A.B. Koenders, Representative elementary volumes for 3D modeling of mass transport in cementitious materials, Model. Simul. Mater. Sci. Eng. 22 (2014) 035001.

[34] S. Dehghanpoor Abyaneh, H.S. Wong, N.R. Buenfeld, Modelling the diffusivity of mortar and concrete using a three-dimensional mesostructure with several aggregate shapes, Comput. Mater. Sci. 78 (2013) 63–73.
[35] F. Nilenius, F. Larsson, K. Lundgren, K. Runesson, Computational homogenization of diffusion in three-phase mesoscale concrete, Comput. Mech. 54 (2014) 461–472.
[36] M. Zhang, G. Ye, K. van Breugel, Multiscale lattice Boltzmann-finite element modelling of chloride diffusivity in cementitious materials. Part I: algorithms and implementation, Mech. Res. Commun. 58 (2014) 53–63.
[37] M. Zhang, G. Ye, K. van Breugel, Multiscale lattice Boltzmann-finite element modelling of chloride diffusivity in cementitious materials. Part II: simulation results and validation, Mech. Res. Commun. 58 (2014) 64–72.
[38] Q. Yuan, C. Shi, G. De Schutter, K. Audenaert, D. Deng, Chloride binding of cement-based materials subjected to external chloride environment – a review, Constr. Build. Mater. 23 (2009) 1–13.
[39] Y. Zhang, M. Zhang, Transport properties in unsaturated cement-based materials – a review, Constr. Build. Mater. 72 (2014) 367–379.
[40] J.-P. Ollivier, J.-M. Torenti, M. Carcassés, Physical Properties of Concrete and Concrete Constituents, John Wiley & Sons, 2012.
[41] C. Steefel, C. Appelo, B. Arora, D. Jacques, T. Kalbacher, O. Kolditz, V. Lagneau, P. Lichtner, K.U. Mayer, J. Meeussen, Reactive transport codes for subsurface environmental simulation, Comput. Geosci. 19 (2015) 445–478.
[42] E. Samson, J. Marchand, K.A. Snyder, Calculation of ionic diffusion coefficients on the basis of migration test results, Mater. Struct. 36 (2003) 156–165.
[43] C.A.J. Appelo, D. Postma, Geochemistry, Groundwater and Pollution, CRC press, 2004.
[44] K. Krabbenhøft, J. Krabbenhøft, Application of the Poisson–Nernst–Planck equations to the migration test, Cem. Concr. Res. 38 (2008) 77–88.
[45] L. Tang, Concentration dependence of diffusion and migration of chloride ions: Part 1. Theoretical considerations, Cem. Concr. Res. 29 (1999) 1463–1468.
[46] L.P. Tang, J. Gulikers, On the mathematics of time-dependent apparent chloride diffusion coefficient in concrete, Cem. Concr. Res. 37 (2007) 589–595.
[47] Q.T. Phung, N. Maes, D. Jacques, E. Jacop, A. Grade, G.D. Schutter, G. Ye, Determination of diffusivities of dissolved gases in saturated cement-based materials, in: F. Dehn, H.-D. Beushausen, M.G. Alexander, P. Moyo (Eds.), International Conference on Concrete Repair, Rehabilitation and Retrofitting IV, CRC Press, Leipzig, Germany 2015, pp. 1019–1027.
[48] Q.T. Phung, Effects of Carbonation and Calcium Leaching on Microstructure and Transport Properties of Cement Pastes, in: Department of Structural Engineering, Ghent University, Belgium, 2015 249.
[49] E. Jacops, G. Volckaert, N. Maes, E. Weetjens, J. Govaerts, Determination of gas diffusion coefficients in saturated porous media: He and CH_4 diffusion in Boom Clay, Appl. Clay Sci. 83–84 (2013) 217–223.
[50] M. García-Gutiérrez, J.L. Cormenzana, T. Missana, M. Mingarro, J. Molinero, Overview of laboratory methods employed for obtaining diffusion coefficients in FEBEX compacted bentonite, J. Iber. Geol. 32 (2006) 37–53.
[51] M. Castellote, C. Andrade, C. Alonso, Measurement of the steady and non-steady-state chloride diffusion coefficients in a migration test by means of monitoring the conductivity in the anolyte chamber - comparison with natural diffusion tests, Cem. Concr. Res. 31 (2001) 1411–1420.
[52] B. Park, S.Y. Jang, J.-Y. Cho, J.Y. Kim, A novel short-term immersion test to determine the chloride ion diffusion coefficient of cementitious materials, Constr. Build. Mater. 57 (2014) 169–178.
[53] M. Castellote, C. Alonso, C. Andrade, G.A. Chadbourn, C.L. Page, Oxygen and chloride diffusion in cement pastes as a validation of chloride diffusion coefficients obtained by steady-state migration tests, Cem. Concr. Res. 31 (2001) 621–625.
[54] S.W. Yu, C.L. Page, Diffusion in cementitious materials: 1. Comparative study of chloride and oxygen diffusion in hydrated cement pastes, Cem. Concr. Res. 21 (1991) 581–588.
[55] J. Crank, The Mathematics of Diffusion, Clarendon Press, 1975.
[56] J.-P.O.L.-O. Nilsson, Fundamentals of transport properties of cement-based materials and general methods to study transport properties, in: G.A.M.G. Alexander, G. Ballivy, A. Bentur, J. Marchand (Eds.),Engineering and Transport Properties of the Interfacial Transition Zone in Cementitious Composites - State-of-the-Art Report of RILEM TC 159-ETC and 163-TPZ 1999, pp. 113–147.
[57] Nordtest, Concrete, Hardened: Accelerated Chloride Penetration (NT BUILD 443), 1995.
[58] L.O. Nilson, Models for chloride ingress into concrete - from Collepardi to today, advances in concrete structural durability, Proceedings of Icdcs2008, 1 and 2, 2008, pp. 36–42.
[59] M. Nokken, A. Boddy, R.D. Hooton, M.D.A. Thomas, Time dependent diffusion in concrete—three laboratory studies, Cem. Concr. Res. 36 (2006) 200–207.
[60] ASTM, ASTM Standard Test Method for Determining the Apparent Chloride Diffusion Coefficient of Cementitious Mixtures by Bulk Diffusion (C 1556-04), 2004.
[61] E.N. European Standard, 12390–11: Testing Hardened Concrete - Part 11: Determination of the Chloride Resistance of Concrete, Unidirectional Diffusion, 2015.
[62] J.-P.T.J.-M.C.M. Ollivier, Physical Properties of Concrete and Concrete Constituents, ISTE/Wiley, London; Hoboken, N.J., 2012
[63] P.A. Claisse, Transport Properties of Concrete: Measurement and Applications, Woodhead Pub, Waltham, MA, 2014.
[64] C. Sun, J. Chen, J. Zhu, M. Zhang, J. Ye, A new diffusion model of sulfate ions in concrete, Constr. Build. Mater. 39 (2013) 39–45.
[65] H.-Y. Moon, S.-T. Lee, H.-S. Kim, S.-S. Kims, Experimental Study on the Sulfate Resistance of Concrete Blended Ground Granulated Blast-furnace Slag for Recycling, Geosystem Engineering, 5, 2002 67–73.
[66] P.J. Tumidajski, I. Turc, A rapid test for sulfate ingress into concrete, Cem. Concr. Res. 25 (1995) 924–928.
[67] T. Luping, L.-O. Nilsson, Rapid determination of the chloride diffusivity in concrete by applying an electric field, ACI Mater. J. 89 (1993) 49–53.
[68] C.C. Yang, S.C. Chiang, L.C. Wang, Estimation of the chloride diffusion from migration test using electrical current, Constr. Build. Mater. 21 (2007) 1560–1567.
[69] O. Truc, J.P. Ollivier, M. Carcasses, A new way for determining the chloride diffusion coefficient in concrete from steady state migration test, Cem. Concr. Res. 30 (2000) 217–226.
[70] NT Build 355, Concrete, Mortar and Cement Based Repair Materials: Chloride Diffusion Coefficient from Migration Cell Experiments, Nordtest Standards Institution, 1995.
[71] NT BUILD 492, Concrete, Mortar and Cement-Based Repair Materials: Chloride Migration Coefficient from Non-Steady-State Migration Experiments, Nordtest, Finland, 1999.
[72] L. Tong, O.E. Gjørv, Chloride diffusivity based on migration testing, Cem. Concr. Res. 31 (2001) 973–982.
[73] L. Tang, L.-O. Nilsson, P.A.M. Basheer, Resistance of Concrete to Chloride Ingress : Testing and Modelling, Spon Press, London; New York, 2012.
[74] C. Andrade, Calculation of chloride diffusion coefficients in concrete from ionic migration measurements, Cem. Concr. Res. 23 (1993) 724–742.
[75] J.G. Cabrera, P.A. Claisse, Measurement of chloride penetration into silica fume concrete, Cem. Concr. Compos. 12 (1990) 157–161.
[76] ASTM, Standard Test Method for Electrical Indication of Concrete's Ability to Resist Chloride Ion Penetration (C1202-97), in, 1997.
[77] X. Lu, Application of the Nernst-Einstein equation to concrete, Cem. Concr. Res. 27 (1997) 293–302.
[78] K.A. Snyder, X. Feng, B.D. Keen, T.O. Mason, Estimating the electrical conductivity of cement paste pore solutions from OH–, K+ and Na+ concentrations, Cem. Concr. Res. 33 (2003) 793–798.
[79] L.Z. Xiao, X.S. Wei, S.N. Wang, Alternating current method to determine chloride diffusion coefficient of hardened paste and concrete, Mag. Concr. Res. 67 (2015) 27–32.
[80] M.d.C.A. Perdrix, R. d'Andrea, Electrical Resistivity as Microstructural Parameter for the Calculation of Reinforcement Service Life, 2011.
[81] V. Baroghel-Bouny, K. Kinomura, M. Thiery, S. Moscardelli, Easy assessment of durability indicators for service life prediction or quality control of concretes with high volumes of supplementary cementitious materials, Cem. Concr. Compos. 33 (2011) 832–847.
[82] O. Sengul, O.E. Gjørv, Electrical resistivity measurements for quality control during concrete construction, ACI Mater. J. 105 (2008) 541–547.
[83] P. Silva, R. Ferreira, H. Figueiras, Electrical resistivity as a means of quality control of concrete–influence of test procedure, in: International Conference on Durability of Building Materials and Components.
[84] R. Spragg, C. Villani, K. Snyder, D. Bentz, J. Bullard, J. Weiss, Factors that influence electrical resistivity measurements in cementitious systems, Transp. Res. Rec. 2342 (2013) 90–98.
[85] A. Delagrave, J. Marchand, M. Pigeon, Influence of microstructure on the Tritiated water diffusivity of mortars, Adv. Cem. Based Mater. 7 (1998) 60–65.
[86] S. Béjaoui, B. Bary, S. Nitsche, D. Chaudanson, C. Blanc, Experimental and modeling studies of the link between microstructure and effective diffusivity of cement pastes, Revue Européenne de Génie Civil 10 (2006) 1073–1106.
[87] S. Numata, H. Amano, K. Minami, Diffusion of tritiated water in cement materials, J. Nucl. Mater. 171 (1990) 373–380.
[88] T. Yamaguchi, K. Negishi, S. Hoshino, T. Tanaka, Modeling of diffusive mass transport in micropores in cement based materials, Cem. Concr. Res. 39 (2009) 1149–1155.
[89] E. Revertegat, C. Richet, P. Gégout, Effect of pH on the durability of cement pastes, Cem. Concr. Res. 22 (1992) 259–272.
[90] V.T. Ngala, C.L. Page, L.J. Parrott, S.W. Yu, Diffusion in cementitious materials: II, further investigations of chloride and oxygen diffusion in well-cured OPC and OPC/30%PFA pastes, Cem. Concr. Res. 25 (1995) 819–826.
[91] P.J. Tumidajski, A.S. Schumacher, S. Perron, P. Gu, J.J. Beaudoin, On the relationship between porosity and electrical resistivity in cementitious systems, Cem. Concr. Res. 26 (1996) 539–544.
[92] H. Ma, D. Hou, J. Liu, Z. Li, Estimate the relative electrical conductivity of C–S–H gel from experimental results, Constr. Build. Mater. 71 (2014) 392–396.
[93] G. Taffinder, B. Batchelor, Measurement of effective diffusivities in solidified wastes, J. Environ. Eng. 119 (1993) 17–33.
[94] B.J. Christensen, T.O. Mason, H.M. Jennings, D.P. Bentz, E.J. Garboczi, Experimental and computer simulation results for the electrical conductivity of Portland cement paste, MRS Online Proc. Libr. 245 (1992) 259–264.
[95] V.T. Ngala, C.L. Page, Effects of carbonation on pore structure and diffusional properties of hydrated cement pastes, Cem. Concr. Res. 27 (1997) 995–1007.
[96] G.-w. Sun, W. Sun, Y.-s. Zhang, Z.-y. Liu, Relationship between chloride diffusivity and pore structure of hardened cement paste, J. Zhejiang Univ. Sci. A 12 (2011) 360–367.
[97] B.H. Oh, S.Y. Jang, Prediction of diffusivity of concrete based on simple analytic equations, Cem. Concr. Res. 34 (2004) 463–480.
[98] T. Hansen, Physical structure of hardened cement paste. A classical approach, Mater. Struct. 19 (1986) 423–436.
[99] S. Bejaoui, B. Bary, Modeling of the link between microstructure and effective diffusivity of cement pastes using a simplified composite model, Cem. Concr. Res. 37 (2007) 469–480.
[100] W.J. McCarter, G. Starrs, T.M. Chrisp, Electrical conductivity, diffusion, and permeability of Portland cement-based mortars, Cem. Concr. Res. 30 (2000) 1395–1400.
[101] M.R. Nokken, R.D. Hooton, Using pore parameters to estimate permeability or conductivity of concrete, Mater. Struct. 41 (2008) 1–16.

[102] I.S. Yoon, S. Hong, T.H.K. Kang, Influence of curing condition and carbonation on electrical resistivity of concrete, Comput. Concr. 15 (2015) 973–987.
[103] N.H. El-Achkar, Non-destructive electrical resistivity measurement technique: evaluation of concrete strengths, in: M. Grantham, V. Mechtcherine, U. Schneck (Eds.), Concrete Solution 2011, CRC Press 2012, pp. 349–357.
[104] J.K. Su, C.C. Yang, W.B. Wu, R. Huang, Effect of moisture content on concrete resistivity measurement, J. Chin. Inst. Eng. 25 (2002) 117–122.
[105] K.M.A. Hossain, M. Lachemi, Corrosion resistance and chloride diffusivity of volcanic ash blended cement mortar, Cem. Concr. Res. 34 (2004) 695–702.
[106] T. Ohama, M. Kawakami, K. Fukuzawa, Polymers in Concrete: Proceedings of the Second East Asia Symposium on Polymers in Concrete (II-EASPIC), College of Engineering, Nihon University, Koriyama, Japan May 11–13, 1997, 1st ed. E & FN Spon, London; New York, 1997.
[107] J.M. Ortega, J.L. Pastor, A. Albaladejo, I. Sanchez, M.A. Climent, Durability and compressive strength of blast furnace slag-based cement grout for special geotechnical applications, Mater. Constr. 64 (2014).
[108] T.H. Wee, A.K. Suryavanshi, S.S. Tin, Influence of aggregate fraction in the mix on the reliability of the rapid chloride permeability test, Cem. Concr. Compos. 21 (1999) 59–72.
[109] V. L'Hostis, B. Larbi, W. Dridi, P. Le Bescop, P. Dangla, L. Petit, R. Gens, Link between microstructure and tritiated water diffusivity in mortars, EPJ Web of Conferences, 56, 2013, p. 01006.
[110] F. Nugue, M.P. Yssorche-Cubaynes, J.P. Ollivier, Innovative study of non-steady-state tritiated water diffusion test, Cem. Concr. Res. 37 (2007) 1145–1151.
[111] A. Delagrave, J.P. Bigas, J.P. Ollivier, J. Marchand, M. Pigeon, Influence of the interfacial zone on the chloride diffusivity of mortars, Adv. Cem. Based Mater. 5 (1997) 86–92.
[112] C.C. Yang, J.K. Su, Approximate migration coefficient of interfacial transition zone and the effect of aggregate content on the migration coefficient of mortar, Cem. Concr. Res. 32 (2002) 1559–1565.
[113] H. Friedmann, O. Amiri, A. Ait-Mokhtar, P. Dumargue, A direct method for determining chloride diffusion coefficient by using migration test, Cem. Concr. Res. 34 (2004) 1967–1973.
[114] NIST, http://ciks.cbt.nist.gov/poresolncalc.html, in: Estimation of Pore Solution Conductivity.
[115] G. Sun, W. Sun, Y. Zhang, Z. Liu, Multi-scale modeling of the effective chloride ion diffusion coefficient in cement-based composite materials, J. Wuhan Univ. Technol-Mat. Sci. Edit 27 (2012) 364–373.
[116] J.-j. Zheng, H.S. Wong, N.R. Buenfeld, Assessing the influence of ITZ on the steady-state chloride diffusivity of concrete using a numerical model, Cem. Concr. Res. 39 (2009) 805–813.
[117] H. Hornain, J. Marchand, V. Duhot, M. Moranville-Regourd, Diffusion of chloride ions in limestone filler blended cement pastes and mortars, Cem. Concr. Res. 25 (1995) 1667–1678.
[118] W.O. Winsauer, J.H.M. Shearin, P.H. Masson, M. Williams, Resistivity of brine-saturated sands in relation to pore geometry, AAPG Bull. 36 (1952) 253–277.
[119] M. Mainguy, C. Tognazzi, J.-M. Torrenti, F. Adenot, Modelling of leaching in pure cement paste and mortar, Cem. Concr. Res. 30 (2000) 83–90.
[120] J.C. Walton, L. Plansky, R.W. Smith, Models for estimation of service life of concrete barriers in low-level radioactive waste disposal, Nuclear Regulatory Commission, Washington, DC (USA). Div. of Engineering; EG and G Idaho, Inc., Idaho Falls, ID (USA), 1990.
[121] P. Pivonka, C. Hellmich, D. Smith, Microscopic effects on chloride diffusivity of cement pastes—a scale-transition analysis, Cem. Concr. Res. 34 (2004) 2251–2260.
[122] B. Bary, S. Béjaoui, Assessment of diffusive and mechanical properties of hardened cement pastes using a multi-coated sphere assemblage model, Cem. Concr. Res. 36 (2006) 245–258.
[123] E. Stora, B. Bary, Q.-C. He, On estimating the effective diffusive properties of hardened cement pastes, Transp. Porous Media 73 (2008) 279–295.
[124] W. Dridi, Analysis of effective diffusivity of cement based materials by multi-scale modelling, Mater. Struct. 46 (2013) 313–326.
[125] X. Liu, R. Lackner, C. Pichler, Highlighting the effect of gel-pore diffusivity on the effective diffusivity of cement paste — a multiscale investigation, in: Y. Yuan, J. Cui, H. Mang (Eds.), Computational Structural Engineering, Springer, Netherlands 2009, pp. 973–981.
[126] P.D. Tennis, H.M. Jennings, A model for two types of calcium silicate hydrate in the microstructure of Portland cement pastes, Cem. Concr. Res. 30 (2000) 855–863.
[127] O. Bernard, F.-J. Ulm, E. Lemarchand, A multiscale micromechanics-hydration model for the early-age elastic properties of cement-based materials, Cem. Concr. Res. 33 (2003) 1293–1309.
[128] G.E. Archie, The Electrical Resistivity Log as an Aid in Determining Some Reservoir Characteristics, in: Dallas Meeting, Dallas, 1941.
[129] K.K. Aligizaki, Pore Structure of Cement-Based Materials: Testing, Interpretation and Requirements, CRC Press, 2005.
[130] B.J. Christensen, T.O. Mason, H.M. Jennings, D.P. Bentz, E.J. Garboczi, Experimental and computer simulation results for the electrical conductivity of Portland cement paste, MRS Online Proc. Libr. 245 (1991) (null-null).
[131] K. Haga, S. Sutou, M. Hironaga, S. Tanaka, S. Nagasaki, Effects of porosity on leaching of Ca from hardened ordinary Portland cement paste, Cem. Concr. Res. 35 (2005) 1764–1775.
[132] J.M. Galindez, J. Molinero, Assessment of the long-term stability of cementitious barriers of radioactive waste repositories by using digital-image-based microstructure generation and reactive transport modelling, Cem. Concr. Res. 40 (2010) 1278–1289.
[133] J.V.D. Lee, L.D. Windt, V. Lagneau, Application of reactive transport models in cement based porous media, in: E. Schlangen, G.D. Schutter (Eds.) International RILEM Symposium on Concrete Modelling - ConMod '08, 2008, pp. 463–470.
[134] D.P. Bentz, E.J. Garboczi, C.J. Haecker, O.M. Jensen, Effects of cement particle size distribution on performance properties of Portland cement-based materials, Cem. Concr. Res. 29 (1999) 1663–1671.
[135] G. Ye, Percolation of capillary pores in hardening cement pastes, Cem. Concr. Res. 35 (2005) 167–176.
[136] G. Ye, K.V. Breugel, Three-dimensional microstructure simulation model of cement based materials, Heron, 48, 2003, pp. 251–275.
[137] E.J. Garboczi, D.P. Bentz, The effect of statistical fluctuation, finite size error, and digital resolution on the phase percolation and transport properties of the NIST cement hydration model, Cem. Concr. Res. 31 (2001) 1501–1514.
[138] D.P. Bentz, O.M. Jensen, A.M. Coats, F.P. Glasser, Influence of silica fume on diffusivity in cement-based materials: I. Experimental and computer modeling studies on cement pastes, Cem. Concr. Res. 30 (2000) 953–962.
[139] S. Torquato, Random Heterogeneous Materials: Microstructure and Macroscopic Properties, Springer Science & Business Media, 2013.
[140] H.M. Jennings, Colloid model of C—S—H and implications to the problem of creep and shrinkage, Mater. Struct. 37 (2004) 59–70.
[141] A.N. Norris, A differential scheme for the effective moduli of composites, Mech. Mater. 4 (1985) 1–16.
[142] P.N. Sen, C. Scala, M.H. Cohen, A self-similar model for sedimentary rocks with application to the dielectric constant of fused glass beads, Geophysics 46 (1981) 781–795.
[143] L. Dormieux, D.D. Kondo, F.J. Ulm, Microporomechanics, John Wiley & Sons, Chichester, West Sussex, England; Hoboken, NJ, 2006.
[144] G. Milton, Concerning bounds on the transport and mechanical properties of multicomponent composite materials, Applied Physics A 26 (1981) 125–130.
[145] S. Bejaoui, H. Peycelon, P.L. Bescop, Determination of the Effective Diffusion Coefficients of Cement Pastes on the Basis of a Simplified Micro/Macro Homogenization Method - Application to the Modelling of Degradation, Euromat, Lausanne, Switzerland, 2003.
[146] E. Stora, Q.-C. He, B. Bary, A mixed composite spheres assemblage model for the transport properties of random heterogeneous materials with high contrasts, J. Appl. Phys. 100 (2006) 084910.
[147] E. Stora, B. Bary, Q.C. He, E. Deville, P. Montarnal, Modelling and simulations of the chemo–mechanical behaviour of leached cement-based materials: leaching process and induced loss of stiffness, Cem. Concr. Res. 39 (2009) 763–772.
[148] P. Halamickova, R.J. Detwiler, D.P. Bentz, E.J. Garboczi, Water permeability and chloride-ion diffusion in Portland-cement mortars - relationship to sand content and critical pore diameter, Cem. Concr. Res. 25 (1995) 790–802.
[149] A.J. Katz, A.H. Thompson, Quantitative prediction of permeability in porous rock, Phys. Rev. B 34 (1986) 8179–8181.
[150] L.M. Schwartz, E.J. Garboczi, D.P. Bentz, Interfacial transport in porous-media - application to DC electrical-conductivity of mortars, J. Appl. Phys. 78 (1995) 5898–5908.
[151] S. Care, Influence of aggregates on chloride diffusion coefficient into mortar, Cem. Concr. Res. 33 (2003) 1021–1028.
[152] S. Care, E. Herve, Application of a n-phase model to the diffusion coefficient of chloride in mortar, Transp. Porous Media 56 (2004) 119–135.
[153] E. Stora, B. Bary, Q.C. He, E. Deville, P. Montarnal, Modelling and simulations of the chemo-mechanical behaviour of leached cement-based materials leaching process and induced loss of stiffness, Cem. Concr. Res. 39 (2009) 763–772.
[154] J.-J. Zheng, X.-Z. Zhou, Effective medium method for predicting the chloride diffusivity in concrete with ITZ percolation effect, Constr. Build. Mater. 47 (2013) 1093–1098.
[155] J.J. Zheng, H.S. Wong, N.R. Buenfeld, Assessing the influence of ITZ on the steady-state chloride diffusivity of concrete using a numerical model, Cem. Concr. Res. 39 (2009) 805–813.
[156] J. Koelman, A. De Kuijper, An effective medium model for the electric conductivity of an N-component anisotropic and percolating mixture, Physica A: Statistical Mechanics and its Applications 247 (1997) 10–22.
[157] E.J. Garboczi, D.P. Bentz, Analytical formulas for interfacial transition zone properties, Adv. Cem. Based Mater. 6 (1997) 99–108.
[158] E. Herve, A. Zaoui, N-layered inclusion-based micromechanical modeling, Int. J. Eng. Sci. 31 (1993) 1–10.
[159] R. Christensen, Mechanics of Composite Materials, Dover, Mineola, NY, 1979.
[160] E. Herve, Thermal and thermoelastic behaviour of multiply coated inclusion-reinforced composites, Int. J. Solids Struct. 39 (2002) 1041–1058.
[161] G. Milton, Concerning bounds on the transport and mechanical properties of multicomponent composite materials, Applied Physics A 26 (2) (1981) 125–130.
[162] Z. Hashin, Thin interphase/imperfect interface in conduction, J. Appl. Phys. 89 (2001) 2261–2267.
[163] B. Bourdette, E. Ringot, J. Ollivier, Modelling of the transition zone porosity, Cem. Concr. Res. 25 (1995) 741–751.
[164] Q.-S. Zheng, D.-X. Du, An explicit and universally applicable estimate for the effective properties of multiphase composites which accounts for inclusion distribution, J. Mech. Phys. Solids 49 (2001) 2765–2788.
[165] F.H. Heukamp, Chemomechanics of Calcium Leaching of Cement-Based Materials at Different Scales: The Role of CH-Dissolution and C-S-H Degradation on Strength and Durability Performance of Materials and Structures, Dept. of Civil and Environmental Engineering, Massachusetts Institute of Technology, 2003.
[166] B. Bourdette, Durabilité du mortier: prise en compte des auréoles de transition dans la caractérisation et la modélisation des processus physiques et chimiques d'altération, 1994.
[167] C. Le Bellego, É. normale supérieure de Cachan, Couplages chimie-mécanique dans les structures en béton attaquées par l'eau: étude expérimentale et analyse numérique, LMT-ENS Cachan, 2001.

[168] D.P. Bentz, E.J. Garboczi, Computer modelling of interfacial transition zone: microstructure and properties, RILEM REPORT (1999) 349–385.
[169] S. Torquato, Random Heterogeneous Materials: Microstructure and Macroscopic Properties, Springer Science & Business Media, 2002.
[170] P.-z. Wong, J. Koplik, J.P. Tomanic, Conductivity and permeability of rocks, Phys. Rev. B 30 (1984) 6606–6614.
[171] J. Zheng, X. Zhou, Analytical solution for the chloride diffusivity of hardened cement paste, J. Mater. Civ. Eng. 20 (2008) 384–391.
[172] A. Delagrave, J. Bigas, J. Ollivier, J. Marchand, M. Pigeon, Influence of the interfacial zone on the chloride diffusivity of mortars, Adv. Cem. Based Mater. 5 (1997) 86–92.
[173] C. Yang, J. Su, Approximate migration coefficient of interfacial transition zone and the effect of aggregate content on the migration coefficient of mortar, Cem. Concr. Res. 32 (2002) 1559–1565.
[174] C. Tognazzi, Couplage fissuration- dégradation chimique dans les matériaux cimentaires: caractérisation et modélisation, in, 1998.
[175] H. Lamotte, A.L. Cocguen, Proprie´te´s de confinement a` long terme des be´tons, CEA Internal Report, NT-SCCD-2002-51, 2002 (in French).